Colombera Luca (Orcid ID: 0000-0001-9116-1800)
Mountney Nigel P (Orcid ID: 0000-0002-8356-9889)

The thickness variability of fluvial cross-strata as a record of dune disequilibrium and palaeohydrology proxy: A test against channel deposits

Luca Colombera[1,2]*, Arnold J.H. Reesink[3,4], Robert A. Duller[5], Victoria A. Jeavons[5], Nigel P. Mountney[2]

1) Dipartimento di Scienze della Terra e dell'Ambiente, Università degli Studi di Pavia, Italy
2) School of Earth and Environment, University of Leeds, UK
3) Lancing College, UK
4) School of Social Sciences and Humanities, Loughborough University, UK
5) Department of Earth, Ocean and Ecological Sciences, University of Liverpool, UK

*) corresponding author: luca.colombera@unipv.it

Associate Editor – Christopher Fielding

Short Title – Dune disequilibrium in fluvial cross-strata

ABSTRACT

Strata produced by fluvial dunes can provide insight into the hydrological regime of ancient rivers. Recent experiments indicate that conditions of disequilibrium between bedforms and formative flows may be inferred from the coefficient of variation of preserved dune cross-set thickness, suggesting that this quantity may act as a proxy for the flashiness of river floods relative to the time required for full bedform translation. To assess whether this idea is applicable to interpretations of the stratigraphic record, this study examines published data relating to more than 2600 cross-sets from 53 sedimentary units of 19 river systems. The presented analyses must not be over interpreted, because the considered rivers span different environmental settings, the data sources are heterogeneous in terms of type and dimensionality, and some variables were established by applying empirical relationships. Yet,

This article has been accepted for publication and undergone full peer review but has not been through the copyediting, typesetting, pagination and proofreading process which may lead to differences between this version and the Version of Record. Please cite this article as doi: 10.1111/sed.13147

significant findings are revealed. Larger rivers exhibit discharge and bedform characteristics that are more conducive to disequilibrium; however, a modest increase in the coefficient of variation of cross-set thickness, $CV(D_{st})$, as opposed to the expected decrease, is seen as a function of river size. Crucially, smaller $CV(D_{st})$ values are not systematically associated with conditions that should favour dune disequilibrium. Meanwhile, only *ca* 25% of the studied examples demonstrate cross-set thickness statistics compatible with quantitative formulations of the autogenic control by variable dune topography – the notion of 'variability-dominated' preservation. These findings indicate that the variability in cross-set thickness may be a poor predictor of discharge variability, perhaps because of the multiplicity of factors controlling dune preservation, such as bedform hierarchy, transport stage and depth-dependent variations in dune disequilibrium. To improve interpretations of cross-stratified deposits, further research is needed to: (i) establish the value of process-to-product models for reverse product-to-process interpretations; and (ii) to define representative samples for preserved dune deposits accounting for temporal and spatial variability in preservation potential.

Keywords: bedform, cross-bedding, cross-set, discharge variability, river, thickness.

INTRODUCTION

Sedimentary strata provide a unique record of past environmental conditions on Earth and other planets. However, interpretations of the preserved sedimentary record rely on our understanding of what is preserved and what is lost over time to erosion. Fluvial deposits, and especially cross-stratified sets formed by migration of subaqueous dunes (Fig. 1A), are well studied in this regard. Key studies span theory (Barrell, 1917; Paola & Borgman, 1991), experiments (Leclair & Bridge, 2001), numerical modelling (Jerolmack & Mohrig, 2005) and field investigations (Lunt *et al.,* 2013). Recent work highlights nuance in the mechanisms of dune cross-strata generation and preservation (Reesink *et al.,* 2015; Leary & Ganti, 2020; Ganti *et al.,* 2020; Das *et al.,* 2022; Lyster *et al.,* 2022). In particular, these recent studies highlight competing controls on bedform preservation and cross-set thickness distributions. Among these factors, special interest has been directed towards the possible role of flood-hydrograph peakedness in controlling dune disequilibrium and resulting cross-set thickness statistics. Leary & Ganti (2020) suggested that the coefficient of variation in dune-scale cross-set thickness can be considered as an indicator of bedform disequilibrium and river flood behaviour applicable to interpretations of the fluvial stratigraphic record. However, the predictive value of cross-set thickness quantifications for studies of river palaeohydraulics and palaeohydrology has yet to be tested. Such a test is needed in view of the wide range of factors that may affect dune preservation as cross-sets of variable thickness.

The aim of this paper is to test the potential value of the variability in dune-scale cross-set thickness as a proxy for bedform disequilibrium and flood-discharge peakedness, as hypothesized by Leary & Ganti (2020), given its significance for palaeohydraulic and palaeohydrological interpretations of the ancient stratigraphic record. In addressing this, consideration is also given to alternative models accounting for dune preservation as cross-stratified sets. The following section provides the scientific background to this work and offers some rationale to the specific objectives of the research.

BACKGROUND

Controls on the thickness variability of dune-scale cross-strata

Sets of cross-stratified sand or sandstone of fluvial origin represent the preserved record of the migration of individual dunes or unit bars, such as transverse bars (Smith, 1974). Individual cross-stratified sets tend to be arranged in cosets (Fig. 1B) produced by the propagation of trains of bedforms on channel floors or bar slopes (Bristow, 1993; Leclair, 2002; Bridge, 2006). Multiple cosets can themselves become amalgamated to form composite stacks of cross-strata. For cross-strata produced by dune migration – the specific focus of this article – the thickness of cross-stratified sets accumulated as in-channel deposits depends on a number of factors. For constant flow conditions and negligible streambed aggradation, the inherent variability in dune topography (scour depth) is generally considered as the main control on thickness distributions via its effect on sediment preservation (Barrell, 1917; Kolmogorov, 1951; Paola & Borgman, 1991), a notion referred to as 'variability-dominated preservation' (Fig. 2A; Reesink *et al.,* 2015). Two additional factors that control cross-set thickness distributions include: (i) the relative rates of deposition and bedform migration, both of which vary significantly in non-uniform flows; and (ii) variations in scour depth linked to temporal changes in river discharge and transport stage (Jerolmack & Mohrig, 2005; Reesink *et al.,* 2015; Leary & Ganti, 2020; Das *et al.,* 2022).

The ubiquitous variations in river width and depth introduce considerable spatial non-uniformity in river flow. For bedforms of a given size, sediment preservation is dictated by the relative rates of streambed aggradation and bedform migration (Sorby, 1859; Bridge, 1997; Jerolmack & Mohrig, 2005). Deposition rates vary across different depositional settings (for example, bar lee slopes, active versus abandoned channels) and this can give rise to spatial differences in preservation potential between and within individual river channels (Reesink *et al.,* 2015). Moreover, bedload transport is often expressed in the migration of bedforms, such that bedform migration and deposition are distinctly dependent upon one another. The coexistence of multiple scales of hierarchically arranged bedforms is expected to create local variability in deposition and migration (Ganti *et al.,* 2020). However, the precise nature of this variability in preservation potential, and the degree to which preserved deposits may be affected by such spatial variability, remain unconstrained.

Sediment preservation may also be affected by temporal flow unsteadiness. Experimental observations suggest that the peakedness of flood hydrographs controls dune disequilibrium and determines the frequency distributions of the resulting cross-strata. On this basis, the coefficient of variation in dune-scale cross-set thickness is considered as a potential proxy for bedform disequilibrium that can be applied to palaeohydraulic interpretations of the stratigraphic record (Leary & Ganti, 2020). However, there are other ways in which flow unsteadiness may control dune disequilibrium and cross-set thickness statistics. For example, the sequence of distinct discharge events of different magnitudes may affect preservation because dune scour depth scales to transport stage (Bradley & Venditti, 2017; Das *et al.,* 2022). It is possible that in some places, such as the thalwegs of perennial rivers, preservation is a direct function of the variability in peak flood discharges (Kleinhans, 2002). Such flood-dependent scour can be limited by the potential presence of pavements and coarser sediments on streambeds (cf. Kleinhans, 2001; Rodrigues *et al.,* 2015). Given the known range in discharge regimes (cf. Fielding *et al.,* 2018), it appears as if the link between discharge and dune preservation may vary across depositional niches and river systems.

Under conditions of equilibrium between the geometry of dunes and the flow that drives their formation and migration – and assuming no streambed aggradation and constant flow (steady state) – the distribution of the thickness of sets of dune-scale cross-strata is controlled by the variability in the depth of dune-trough scour (Paola & Borgman, 1991; Fig. 2A). By contrast, under conditions of unsteady flow the thickness of cross-sets may also reflect the way in which bedform adjustment to flow conditions lags behind changes in flow, resulting in hysteresis (cf. Allen, 1973, 1976b; Gabel, 1993; Julien *et al.,* 2002; Reesink *et al.,* 2018; Bradley & Venditti, 2021; Lisimenka *et al.,* 2022). For the same water discharge, larger dunes exist during the falling stage of a flood compared to the rising stage. There are multiple causes of dune hysteresis, including: (i) the relaxation timescale over which mass redistribution occurs over and among dunes (Allen & Friend, 1976); (ii) fundamentally different modes of bedform growth and decay, with bedform amalgamation through rising stage being more rapid than the cannibalization of larger dunes by smaller dunes during falling stage (Fig. 2B; Martin & Jerolmack, 2013; Reesink *et al.,* 2018; Myrow *et al.,* 2018); (iii) the existence of a phase lag between water depth and flow velocity during the passage of flood waves, since water depth and flow velocity shape bedform geometry in different ways (Reesink *et al.,* 2018); and (iv) temporal variations in sediment transport rates because skin friction changes as a function of the form drag created by the evolving bedforms (cf. Wilbers & Ten Brinke, 2003; Paarlberg *et al.,* 2010). Dune hysteresis varies spatially because the controlling variables, such as discharge, depth and slope, vary spatially within and between river systems. Additionally, experimental evidence indicates that processes of dune adaptation, such as enhanced sediment bypass, have the potential to change the nature and recurrence of dune scour, which ultimately determines the thicknesses of the preserved dune sets (Reesink *et al.,* 2018; Naqshband *et al.,* 2021).

Dune disequilibrium and preservation

Analysis of the role of flow unsteadiness on dune preservation requires a measure of disequilibrium between flow and dunes. To describe the degree of bedform disequilibrium, a dimensionless quantity called bedform equilibrium number (T^*) was proposed by Myrow *et al.* (2018; cf. 'time ratio' of Allen 1976a; Allen & Friend, 1976; see also: Martin & Jerolmack, 2013). The bedform equilibrium number is defined as: $T^* = T_f/T_t$, where T_f is the characteristic duration of certain flow conditions against which equilibrium is considered, and T_t is the bedform turnover time. The bedform turnover time (T_t) is the length of time required for the sediment volume within a bedform to be fully displaced, which is equivalent to the ratio between bedform spacing, or wavelength (λ), and celerity (c). The smaller the value of T^*, the faster the flow is changing relative to the changeover in bedform geometry and, hence, the greater the expected form-flow disequilibrium. Experimental data indicate that equilibrium may be reached over a timescale that is *ca* 10 T_t for rising flows, during which smaller bedforms grow by merging (Martin & Jerolmack, 2013). Conversely, during receding flow stages, when larger bedforms become cannibalized, the time required to achieve equilibrium conditions is instead close to (i.e. about one time) the bedform turnover timescale (Martin & Jerolmack, 2013; Myrow *et al.,* 2018). Nonetheless, T* presents an objective and measurable proxy for disequilibrium that enables a critical analysis of the role of reach-scale disequilibrium as a control on bedform preservation.

Crucially, T^* and the nature of bedform equilibrium are related to the spread and modality of the distribution of dune size. The concept of bedform turnover time (T_t) is based on a single representative dune size, and hence better designed for trains of bedforms with geometries that remain statistically stationary in space and time. However, in reality, the size of dunes varies temporally and across a streambed. When T^* is applied to describe dunes whose geometry changes through time, it is unclear which dune size should be picked to represent the temporal variation, although average values have been considered in earlier studies (Martin & Jerolmack, 2013; Leary & Ganti, 2020). Similarly, it is not well understood what bedform size is representative when dune populations exhibit a greater spread in size, especially considering that smaller T^* values (i.e. increased disequilibrium, under which preservation potential may be greater; Leary & Ganti, 2020) may be associated with more variable dune heights (Allen 1976a). In fact, it is often implicitly considered that variable dune sizes are characteristic of a disequilibrium condition (Myrow *et al.,* 2018). The T^* concept is not readily applicable for regions of non-uniform (expanding) flow, where the highest rates of deposition ought to enhance preservation potential whilst simultaneously creating spatial trends in dune size that prevent the identification of a representative average (Rubin & Hunter, 1982; Reesink *et al.,* 2015). Additionally, T^* does not take into consideration the relative contributions of the multiple processes that drive the adaptation of dunes in non-uniform flows, nor the spatial variability in dune adaptation observed in natural rivers. Despite these complications, T^* is used herein because it presents an objective parameter for the description of dune adaptation at a river-reach scale, which matches the available data on preserved dune sets against which it is compared.

Bedform disequilibrium occurs when existing dunes are too large or too small for a given discharge and transport stage, compared to the size expected under equilibrium for that same discharge (Unsworth *et al.,* 2018). During such times, dynamic flow-form feedback processes interplay to redistribute sediment over and among dunes (Reesink *et al.,* 2015). Flood durations vary greatly among rivers, ranging from the flashy discharge that may be characteristic of ephemeral dryland fluvial systems to long-lived floods of large perennial rivers in certain climates (cf. Serinaldi *et al.,* 2018). The duration of prevailing flow conditions (T_f), as portrayed by a flood hydrograph, presents a direct control on bedform disequilibrium. In an idealized, unrealistic scenario where flood events are approximated by step changes in water discharge (i.e. experimental conditions), T_f can be assumed as equal to the duration of the flood itself (see Myrow *et al.,* 2018). The bedform turnover time, T_t, is also dependent on water discharge history as it is linked to bedform hysteresis. Bedform turnover time T_t tends to be larger for phases of bedform decay during the falling stage because bedforms tend to be larger whilst sediment transport rates are reduced (Allen, 1976a; Jones, 1977; Leary & Ganti, 2020). The rate of change in water discharge during flood recession is therefore a particularly important driver of disequilibrium, as highlighted by the observation that bedform hysteresis is more pronounced in 'fast' compared to 'slow' flood events (Fig. 2C; Martin & Jerolmack, 2013).

The preservation of bedforms is dependent on flow stage in a number of ways. Firstly, the regions where erosion and deposition take place within a river vary depending on stage (Bridge, 1993; Szupiany *et al.,* 2012; Hackney *et al.,* 2018). This implies that some areas are dominated by progressive erosion (cf. Gilluly, 1969), some are 'variability-dominated', and others yet may be dominated by deposition (Reesink *et al.*, 2015). The net effect on preservation of spatial variations in sediment transport within rivers is not fully understood. Nonetheless, flow unsteadiness, where combined with spatial variability in sediment transport, may result in *increased* variability in preserved set thicknesses within a given river system. Secondly, falling-stage bedforms tend to be preferentially preserved, since the deposits of the rising stage can be reworked by the ensuing peak flows when dunes are larger and scours are deeper (Jones, 1977). Thus, the deposits of receding flows are more likely to be preserved, and this factor should be pronounced when the receding stages are associated with greater dune size and form roughness and decreased water surface slopes and sediment transport rates, which is the case for most alluvial rivers. Thirdly, the scour depth is affected by the degree to which bedforms are in disequilibrium with their formative flows. At conditions of disequilibrium, bedforms adapt to the flow through the redistribution of sediment over and among successive bedforms (Reesink *et al.,* 2018). Sediment redistribution happens through multiple processes, including local increases in scour and bedform migration that determine local preservation potential (Paola & Borgman, 1991). The likely increased variability in dune size and scour during times of disequilibrium has the potential to *increase* the variability in preserved dune-set thickness. Fourthly, if dunes have less time to develop during short-lived floods, it is less likely that they will reach greater sizes and develop the deeper scours (e.g. Amsler & Garcia, 1997) that would enhance preservation. If greater form-flow disequilibrium is linked to more limited dune development, floods with shorter durations could result in a *decreased* variability in preserved dune-set thickness. Thus, although the precise mechanics of dune preservation are not yet fully understood, it is clear that there can be different competing relations between dune preservation and the dynamic development of form-flow (dis-)equilibrium.

Cross-set thickness variability as a palaeohydraulic indicator

In their benchmark study of the dependency between dune preservation and flow unsteadiness, Leary & Ganti (2020) propose the coefficient of variation (ratio of standard deviation to mean) of the preserved dune sets, $CV(D_{st})$, as an indicator of the rapidity of flood-discharge variations relative to the speed of bedform adjustment to flow changes. The model for 'variability-dominated preservation' proposed by Paola & Borgman (1991), predicts that distributions in cross-set thickness resulting autogenically from migration of trains of dunes of variable relief are characterized by $CV(D_{st})$ values of *ca* 0.88, a quantity supported by experimental findings from flume studies (Ganti *et al.,* 2013). According to the study of Leary & Ganti (2020), values of $CV(D_{st})$ that are markedly lower than 0.88 are indicative of bedform-flow disequilibrium. For a given value of dune turnover time, smaller values of $CV(D_{st})$ are expected for the deposits of floods with more abrupt recessions, based on the assumption that receding flows of shorter duration will produce dune cross-sets of relatively less variable thickness because less time is afforded to achieve equilibrium between bedforms and flow conditions. Based on the findings of Leary & Ganti (2020), dune deposits produced by peaked flood hydrographs, particularly those of rivers subject to flash floods, may therefore be expected to be characterized by reduced variability (relative to mean values) in cross-set thickness compared with the deposits of rivers with longer and slower flood recessions. This hypothesis has implications for our ability to read the stratigraphic record. In principle, quantification of $CV(D_{st})$ can be employed alongside established approaches that use other cross-set thickness statistics (e.g. Leclair & Bridge, 2001) to make interpretations of river palaeohydraulics and palaeohydrology for ancient successions (cf. Wang *et al.,* 2020; Hartley & Owen, 2022; Lyster *et al.,* 2022; McLeod *et al.,* 2023).

In their flume-based study, Leary & Ganti (2020) use the temporal duration of flood recession (i.e. time from peak flood to base flow) as a measure of formative-flow timescale, T_f, and indicate that bedform disequilibrium of a river reach can be assessed on the basis of discharge data and knowledge of characteristic bedform size and celerity (Leary & Ganti, 2020). Because T_t is inherently dependent on bedform scale, disequilibrium and increased preservation may be prevalent in larger river systems characterized by longer timescales of dune decay (Myrow *et al.,* 2018; Leary & Ganti, 2020). However, T_f is expected to vary in concert with T_t, since river reaches with smaller and steeper catchments tend to have shorter falling hydrograph limbs (Chorley, 1969; Davie & Quinn, 2019). Thus, the way in which disequilibrium may vary systematically with the scale of a river system warrants further systematic investigation.

In this paper, an examination is made of the hypothesis that the coefficient of variation of the thickness of dune-scale cross-sets, $CV(D_{st})$, can be used to make inferences of hydrograph peakedness relative to dune turnover time, and therefore, of the extent to which *$CV(D_{st})$* can be used as a proxy for discharge variability at the flood-event scale. This is accomplished by assessing the characteristics of recent dune deposits of several modern rivers for which relevant hydraulic conditions are either known or can be inferred with some confidence.

DATA AND METHODS

Characterization of fluvial strata

Data on the thickness of sets of cross-bedded sands, or descriptive statistics thereof, have been derived from the published scientific literature. Thickness data on over 2600 cross-sets, relating to 53 sedimentary units from 19 rivers, were obtained from 26 literature sources (Table 1). The true total number of cross-sets included in the datasets is unknown because summary statistics (mean and standard deviation) of a sample of unspecified size were reported in one case. For this analysis, the sets of cross-bedded sands were grouped by the higher-scale sedimentary units in which they reside. These units do not typically correspond to cosets, but rather, in most cases, to sedimentary bodies that may differ with respect to their architecture and subenvironment of origin. These units may represent channel fills or barforms of different types (for example, point bars, braid bars; cf. architectural elements of Miall, 1985; Colombera *et al.,* 2013), which may include amalgamated sets of cross-strata produced by different floods. This approach to the aggregation of cross-set data is not ideal for testing the influence of event-scale discharge variability on the thickness distribution of cross-strata, for which data aggregation by cosets produced by individual floods would be more appropriate. However, such practice enables an assessment of the value of analysing *$CV(D_{st})$* data in the manner exemplified by Leary & Ganti (2020) in their application to the rock record, and is in line with recent analyses of stratigraphic successions (cf. Wang *et al.,* 2020; Hartley & Owen, 2022; Lyster *et al.,* 2022; McLeod *et al.,* 2023). In total, data on 53 sedimentary bodies (lithosomes) containing at least six sets of cross-bedding each are available. Given the scope of the theory being tested (Leary & Ganti, 2020), only sets of cross-stratified sands of presumed dune origin were included. Cross-sets were excluded from the dataset in cases where they were explicitly reported as the product – observed or interpreted – of migration of unit bars (cf. Reesink *et al.,* 2014; Herbert *et al.,* 2020); the term 'unit bar' is used here to refer to bars with slip-faces whose propagation generates cross-stratification at a scale similar to that of cross-strata produced by dunes, such as transverse bars. No sets of cross-stratification were removed from the dataset based on reinterpretation of their origin; only interpretations provided by the original authors of the literature data sources were considered.

The thickness of individual cross-stratified sets was, in most cases, measured from one-dimensional sedimentological sections, two-dimensional sections, or graphs of thickness data; in some cases, thickness statistics were derived from tables or text. The cross-sets were originally described in studies of outcrops, cores and PES (parametric echo sounder) acquisitions (Table 1). All thickness values are necessarily underestimations of the true maximum thickness of each set, since the three-dimensional geometry of each set is unknown (Fig. 3). On 2D panels (cf. Leary & Ganti, 2020), the largest observed thickness of each set was recorded, which is a closer estimate of true maximum thickness than the thickness captured by 1D vertical sections (Fig. 3). This approach was chosen because the extraction of 1D samples from 2D panels would require the arbitrary exclusion of a number of sets, given the limited lateral extent of some sets relative to the outcrop exposures.

Characterization of river attributes

A range of attributes were recorded that describe the river systems or the specific river reaches at the study sites. The hydraulic geometry of present-day river channels is characterized by values of mean bankfull depth and bankfull width derived from the empirical database of Andreadis *et al.* (2013), which was itself compiled on the application of power-law relationships between estimated discharge and channel width and depth (Moody & Troutman, 2002). These values are in some cases corroborated by bathymetric observations; however, to ensure consistency, only the empirical estimations of Andreadis *et al.* (2013) were used in all subsequent quantifications. Water-surface slopes were extracted from topographic datasets and literature sources and employed as approximations of streambed gradients. Values of drainage-basin area and mean annual water discharge and water-discharge statistics based on hydrographs of monthly and daily flow were extracted from a variety of sources, including: (i) the scientific literature; (ii) technical reports by the Environmental Protection Agency (EPA) and the Inland Waterways Authority of India (IWAI); and

(iii) hydrological databases of the Global Runoff Data Centre (GRDC) and the United States Geological Survey (USGS). All discharge data refer to and were originally acquired from gauging stations located along or in the vicinity of the study reaches. See Supplementary Information S2.

Determination of bedform characteristics

The grain size of the studied cross-bedded sands is assumed to be the grain size of their original bedforms. However, the morphometry of the formative bedforms is unknown; hence, the geometry of bedforms observed on the modern channel floors during bathymetric acquisitions is considered as a representative proxy, where data are available.

The calibre of streambed sediment was characterized in terms of median grain size (D_{50}), based on data derived from the literature data sources. From these sources, stated D_{50} values were recorded where possible, else mid-values of the dominant grain-size class of cross-bedded sets of each lithosome were considered as representative values (for example, 0.75 mm for coarse sands, i.e. the mid-value of the 0.5–1.0 mm range).

Bedform geometry is characterized in terms of mean dune height (h) and wavelength (λ). Data on dune height and wavelength based on bathymetric observations were compiled from the scientific and technical literature, but are only available for some of the case studies (12 river reaches; Table 1). In addition, for all cases, mean dune height and wavelength were estimated by applying the empirical relationships proposed by Bradley & Venditti (2017) based on regression of flume and river data; these relationships were employed using values of mean bankfull depth (H_{bf}) from Andreadis *et al.* (2013), as follows:

$$\begin{cases} h = 0.23{H_{bf}}^{0.91} & H_{bf} \leq 2.5\ m \\ h = 0.13{H_{bf}}^{0.94} & H_{bf} > 2.5\ m \end{cases}$$

$$\lambda = 5.22{H_{bf}}^{0.95}$$

Where values of mean bankfull depth were not available in the database of Andreadis *et al.* (2013) – i.e. for sites at latitudes higher than 60° (Tana River) – data were derived from the literature (Lotsari *et al.,* 2010). For consistency, mean values of dune height and wavelength for all 19 rivers were derived based on the application of the equations of Bradley & Venditti (2017). Doing so also ensures that all of the data relate to a bankfull flow stage, consistently across all examples. This approach to the determination of a representative dune geometry permits to obtain individual average values for each studied reach, where in practice superimposed bedforms with different morphometric characteristics may exist.

Determination of bedform turnover timescales

Representative values of bedform turnover timescales (T_t) were estimated based on values of mean bedform wavelength and celerity (c), as: $T_t = \lambda/c$.

Alternative values of bedform celerity were obtained by adopting the two following alternative approaches.

1 Application of the empirical relationship of Mahon & McElroy (2018), based on their analysis of data compiled by Lin & Venditti (2013), which allows estimating bedform migration rate from reach-averaged longitudinal channel slope (S), as follows:

$$\log(c) = 0.6113 + 1.305 \cdot \log(S)$$

2 Estimation of bedform celerity from unit sediment flux [i.e. sediment flux per unit channel width (m^2/s)] and mean dune height (cf. Simons *et al.* 1965; Myrow *et al.* 2018), as:

$$c = q_s/h\beta$$

where q_s is the unit sediment flux and β is a shape factor with constant value of 0.6 for river dunes. To obtain representative values of unit sediment flux, alternative sets of sediment-transport relationships were applied. These relationships are formulated as follows (Lajenuesse *et al.,* 2010):

Engelund & Fredsøe (1976), $q_s = 18.74(\tau_* - \tau_{*c})(\sqrt{\tau_*} - 0.7\sqrt{\tau_{*c}})$, $\tau_{*c} = 0.05$

Ashida & Michiue (1973), $q_s = 17(\tau_* - \tau_{*c})(\sqrt{\tau_*} - \sqrt{\tau_{*c}})$, $\tau_{*c} = 0.05$

Meyer-Peter & Müller (1948), $q_s = 8(\tau_* - \tau_{*c})^{\frac{3}{2}}$, $\tau_{*c} = 0.047$

where τ_* is the Shields number and τ_{*c} is the critical Shields stress. The equation by Meyer-Peter & Müller (1948) was only used for D_{50} values coarser than 0.75 mm (upper coarse sand). These empirical relationships were applied taking the following steps: (i) computing a Shields stress for bankfull conditions, assuming normal flow, as: $\tau_* = H_{bf}S/RD_{50}$, where S is the water-surface slope (cf. Czapiga *et al.,* 2019, and references therein), and R is the submerged specific gravity of sediment; (ii) determining the skin-friction component of the Shields stress to account for form drag due to the presence of bedforms under lower flow regime conditions, in the way explained by Wright & Parker (2004; cf. Engelund & Hansen, 1967), as: $\tau_{*sk} = 0.06 + 0.7(\tau_* F_r^{0.7})^{0.8}$. F_r is the Froude number, defined as: $F_r = u/\sqrt{gH}$, where u denotes flow velocity and H denotes flow depth; F_r values were estimated for bankfull conditions based on flow velocities obtained from: (i) data on bankfull discharge or on two-year flood discharge; and on (ii) channel bankfull areas from the database of Andreadis *et al.* (2013).

Data on bedform celerity based on bathymetric surveys were additionally gathered from the literature, but these data are only available for ten of the 19 studied rivers (Table 1).

Determination of flood recession timescales

Values of flood recession timescales (used here to constrain T_f) were obtained for either the flood that caused deposition of the cross-bedded sets, or as the average falling-limb durations of several historical floods recorded at gauging stations in the proximity of the study sites. The flood hydrograph of the formative flood of the deposits could only be determined for a single case study (Powder River; Ghinassi & Moody, 2021). In all other cases, values of flood recession timescales were derived from either the published literature or by statistical analysis of daily discharge data, computing mean values for multiple events with a clear hydrograph slope break (29 floods on average per study reach). Data on flood recession time could not be sourced for the South Fork of the Madison River: the T_f value for the Madison River in the same area was tentatively applied to the South Fork by analogy of catchment size, terrain, climate and geographic location.

Limitations

This study is affected by several notable limitations.

The dataset is heterogeneous in terms of dimensionality and resolution, because it includes observations based on both 1D and 2D data types, obtained from examination of outcrops, vibracores and PES lines. Thus, separate analyses of 1D and 2D datasets have been undertaken. Thinner sets may not be resolvable on PES sections with decimetre-scale resolution (Sambrook Smith *et al.,* 2013), whereas 1D data types will tend to yield smaller estimations of the true maximum thickness of a set. Dataset size also varies considerably across the case studies.

Relating cross-set-thickness statistics to the specific formative conditions of the cross-bedded deposits was only possible in a single instance. In all other cases, statistics of the deposits were related to attributes of the rivers in the present day; yet, present-day conditions might not be representative of formative conditions. In view of millennial-scale changes in climate and river hydrology, this is especially problematic for older deposits, some of which are as old as late Pleistocene in age (River Loire, Table 1). Nevertheless, some of the key attributes considered in this study are likely to have changed little through the considered time spans (for example, reach gradient, employed as predictor of dune celerity). Moreover, because descriptive statistics of cross-set thickness do not reflect grouping by cosets, the coefficients of variation of the considered samples reflect variability across cosets in addition to variability within cosets, i.e. are likely to also record temporal variability in flow conditions across different flood events. Nonetheless, analyses are undertaken by considering average conditions of the river reaches, rather than the specific conditions at time of deposition, and by grouping sets that may occur in different cosets. This allows testing the value of using particular observations on cross-set thickness that may only be representative of special conditions for given times and locations to make general inferences on river hydrology (cf. Leary & Ganti, 2020; Wang *et al.,* 2020; Hartley & Owen, 2022; Lyster *et al.,* 2022; McLeod *et al.,* 2023). In this regard, it is particularly significant that the computed T^* values merely represent a measure of the likelihood of accumulation under conditions of flow-bedform disequilibrium in the studied river reaches.

A further issue exists in that the chosen samples represent the products of sediment accumulation in different depositional niches of variable bathymetry, where a morphodynamic hierarchy (*sensu* Ganti *et al.,* 2020) may exist, and deposition and preservation under inter-flood low-flow conditions may be dominant. Additionally, the chosen approach does not account for the potential presence of superimposed bedforms, which may affect statistics of dune attributes disproportionately relative to their preservation potential. This approach also disregards temporal variations in bedform geometry and celerity through flood events. Adopting the timescale of flood recession as a measure of formative-flow duration T_f is also a major simplification (cf. Myrow *et al.,* 2018), especially since flow conditions can change significantly during waning flow; yet, this was done because it enables a test of the importance of flood hydrograph shape on cross-set thickness distributions (cf. Leary & Ganti, 2020). The approaches employed to estimate representative values of T_t are also subject to fundamental uncertainties regarding: (i) the predictive power of the empirical relationships that were applied; and (ii) the degree to which the considered quantities may be representative of the conditions under which the deposits were formed. For example, some of the predictive relationships are principally based on flume data (Bradley & Venditti, 2017; Mahon & McElroy, 2018), whereas the assumption that a two-year flood may be representative of bankfull conditions (cf. Andreadis *et al.,* 2013) may not be applicable to rivers subject to infrequent major floods. Finally, the considered cross-set statistics will not account for the effects of future sediment reworking on the long-term preservation of the studied deposits.

RESULTS

Dataset summary

Cross-set thickness statistics vary according to the type of observation, as expected (Fig. 4; cf. Fig. 3). On average, observations on 2D sections yield values of cross-set thickness that are larger (mean: 0.31 m versus 0.26 m) and collectively more variable (standard deviation: 0.46 m versus 0.25 m) than those made on 1D sections. These results do not arise due to some bias in the sampling of rivers of different sizes: in fact, the 1D data are associated with rivers with slightly larger catchment areas, on average (mean values: 556,406 km^2 versus 386,060 km^2). Variability is also observed in the shape of cross-set thickness distributions (Fig. 5). In some cases (Brahmaputra, Mississippi), breaks in slope can be identified on cumulative distribution functions, which might reflect the sampling of different populations; this may indicate that cross-stratification arising from unit-bar migration is included in these examples alongside the products of river dunes. Overall, the dataset covers a broad range of river systems in terms of scale and hydrology (Fig. 6; see also Supplementary Fig. S1): six orders of magnitude in catchment size, five orders of magnitude in mean yearly water discharge, and marked differences in both flood-recession durations and discharge seasonality. As a measure of seasonality, the ratio between the mean discharge of the month with highest discharge divided by the mean annual discharge is considered (Leier *et al.,* 2005); this quantity ranges from 1.09 to 5.33 in the studied rivers. Thus, the data relate to a suitable range of conditions to test the applicability of the 'variability-dominated' preservation model and the potential control by flood-discharge variability. All data and estimations reported in this study are included in the supplementary material (Supplementary Information S2).

According to the 'variability-dominated' model of Paola & Borgman (1991), the variance in cross-set thickness is predicted theoretically to yield $CV(D_{st})$ values of *ca* 0.88. The majority of studied examples are characterized by $CV(D_{st})$ values lower than 0.88 (94% of groups of cross-sets) and outside of the range that is commonly considered for variability-dominated preservation (75% of cross-set groups), i.e. 0.88 ± 0.3 (Bridge, 1997; Leclair *et al.,* 1997). This indicates that approximately a quarter of the cases match the variability-dominated model for dune preservation (Paola & Borgman, 1991). The studied distributions of cross-set thickness tend to exhibit positive skewness (90% of cases; mean: 1.04) and positive excess kurtosis (61% of cases; mean: 1.72), but they are not as skewed (skewness = 1.53) or tail-heavy (excess kurtosis = 3.22) as predicted theoretically by Paola & Borgman (1991). However, the groups of cross-sets with $CV(D_{st})$ values in the 0.58 to 1.18 range (25% of observations) are characterized by larger values of skewness (mean: 1.79) and excess kurtosis (mean: 4.94).

River-system characteristics: observations and assessment of predictions

Some variables considered in this study are estimated from empirical relationships, not measured; these include mean bankfull depth and the geometry and migration rate of formative dunes. The direct use of these variables in statistical analyses should therefore be avoided. Instead, to derive general insight from analyses involving empirical estimates, it is possible to: (i) assess empirical predictions against field data; (ii) perform statistical analyses involving cross-set thickness statistics and river characteristics based on the small number of available observations; and (iii) establish whether quantifications that are made employing empirical predictions match corresponding quantifications based on observations.

Predictions of average dune height and wavelength at bankfull conditions based on application of the empirical relationships by Bradley & Venditti (2017) are compared against data on observed dune morphometry (Fig. 7); the latter quantities are representative of the flow stages at which bathymetric surveys were undertaken, and so some discrepancy with predictions for bankfull flow is expected. The goodness of fit between the predicted values and the field measurements is expressed by mean absolute errors (MAEs) equal to 0.26 m for dune height (N = 15) and to 18.9 m for dune length (N = 13).

Estimated values of representative bedform turnover timescales based on the two alternative approaches – that is, by employing values of dune celerity estimated from either channel slope (Mahon & McElroy, 2018) or sediment flux (Simons, 1965) – return consistent results in relative terms (Fig. 8). Because of the variables involved in the estimations, both approaches return values of bedform-turnover times that are inversely proportional to the longitudinal stream gradient. However, it must be considered that unit sediment-flux predictions are additionally scaled to quantities that themselves tend to covary with the riverbed gradient (flow depth and grain size). In general, T_t values based on estimated dune celerity predicted from channel slope tend to be larger compared to corresponding predictions based on unit sediment flux (Fig. 8). When T_t predictions are compared against T_t values based on observed bedform geometries and migration rates (Fig. 9), it is observed that T_t estimations based on rates of sediment flux tend to match observations more closely than T_t estimations based on channel slope (MAEs equal to 20.9 d versus 55.0 d).

Both the bedform-turnover and the flood-recession timescales are expected to increase with river system size, because larger rivers tend to have both larger dunes migrating at a slower rate (cf. Lin & Venditti, 2013; Mahon & McElroy, 2018) and broader flood hydrographs (Chorley, 1969; Davie & Quinn, 2019). Indeed, positive correlations are seen between log-transformed values of flood-recession timescales and the logarithms of both river drainage-basin area (Pearson's R = 0.651, p-value = 0.0004, N = 25) and mean annual water discharge (R = 0.725, p = 0.0004, N = 25). Positive correlations are also seen between log-transformed values of bedform turnover times based on dune data and of both river drainage-basin area (R = 0.771, p = 0.0055, N = 11) and mean annual water discharge (R = 0.727, p = 0.0112, N = 11). Positive scaling between T_t and river-system size is also observed for T_t values predicted by applying empirical relationships for inferring dune celerity based on both streambed gradient and unit sediment flux. It is then important to understand how T_t and T_f vary in relative terms across river systems of different scales, to establish how the prevalence of bedform disequilibrium conditions may vary as a function of river size. In both field observations and estimations based on empirical relationships, T_t varies over a broader range and increases with river-system scale more rapidly, compared to T_f. Modest negative correlations are seen between log-transformed values of T^* based on observed dune celerity and geometry and log-transformed values of both catchment size (R = −0.596, p = 0.0535, N = 11) and mean yearly discharge (R = −0.547, p = 0.0816, N = 11). A record of bedform disequilibrium may therefore be more likely for larger rivers. Of the studied river reaches, T^* estimated using field observations takes a value smaller than unity in a single case (Paraná). T_t values based on estimations made by applying empirical relationships for dune celerity based on sediment flux and channel slope are also in most cases smaller than T_f values (Fig. 10). T^* estimations based on inference of dune celerity from streambed gradient tend to be consistently lower than values based on dune observations (Fig. 11), with a single exception (South Saskatchewan). The same T^* estimations also tend to match T^* values based on field data on dune geometry and velocity slightly less accurately than T^* estimations based on inferred bankfull sediment flux (MAEs equal to 36.5 versus 33.5; Fig. 11). The values of T^* for the same river systems reported by Leary & Ganti (2020) also represent underestimations relative to those calculated herein based on dune data (Fig. 11); however, some of the specific river reaches to which these values refer are not the same (for example, Mississippi).

Test of $CV(d_{st})$ as palaeohydrological proxy

To determine the value of the coefficient of variation (i.e. the ratio of standard deviation to mean) of cross-set thickness, $CV(d_{st})$, as a palaeohydrological proxy (Leary & Ganti, 2020), a test is first made of the fundamental assumptions that underpin its supposed predictive value.

Some moderate positive correlation is seen between log-transformed values of $CV(d_{st})$ and T_t, where the latter is determined based on observations of average dune size and celerity (Pearson's R = 0.641, p-value = 0.0001, N = 30; Fig. 12). The vast majority of these data are from 1D samples of cross-strata (N = 23), for which the same relationship is seen (R = 0.694, p = 0.0002). This observation is counter to the intuition that more rapid bedform turnover should result in more variable thickness distributions (Leary & Ganti, 2020). This finding is further supported by quantifications of T_t based on application of empirical relationships for estimating bedform celerity from channel slope and sediment flux (N = 53; Fig. 12). Positive correlation, albeit weaker, is also seen between log-transformed values of $CV(d_{st})$ and T_f (R = 0.351, p = 0.0099, N = 53; Fig. 13). This observation is in accord with the hypothesis that more rapid flood recessions should result in less variable cross-set thickness distributions (Leary & Ganti, 2020). However, among 1D datasets, this correlation (R = 0.485, p = 0.0043, N = 33) is in part determined by three $CV(d_{st})$ outliers related to the Rio Paraná; these data are peculiar, in that they are based on lacquer peels enabling measurements at very high resolution and incorporate a large number of fully preserved dunes (Reesink *et al.,* 2014). No significant correlation is observed for 2D datasets (R = 0.174, p = 0.4621, N = 20). The aforementioned notably large $CV(d_{st})$ values describe deposits associated with the only river reach (Paraná upstream of the confluence with the Paraguay; Reesink *et al.,* 2014) characterized by T^* values (determined from field-based dune measurements) less than one (mean T^* value: 0.612, N = 30; Fig. 14). Data on the three studied sedimentary bodies from this reach, for which interpreted unit-bar-scale cross-strata have been removed (cf. Reesink *et al.,* 2014), return the only $CV(d_{st})$ values larger than one in the dataset; at reach-scale, however, a $CV(d_{st})$ value of 0.833 is calculated. When relationships between log-transformed values of $CV(d_{st})$ and T^* estimations are examined, moderate negative correlations are seen between $CV(d_{st})$ and T^* based on average dune celerity estimated from unit sediment flux or channel slope, and on field data on dune morphology and celerity (Table 2; Fig. 14A to C). However, no significant relationship is observed when 2D datasets are separately analysed (Table 2). Similar results are seen if T^* values drawn from Leary & Ganti (2020) are applied instead (all data: R = −0.648, p = 0.0003, N = 27; 2D data: R = −0.022, p = 0.9644, N = 7; Fig. 14D). In parallel with these trends, the $CV(d_{st})$ of the deposits of larger rivers tend to be higher (Fig. 14): modest positive correlations are seen between logarithmic transformations of $CV(d_{st})$ and both catchment size (R = 0.466, p = 0.0004, N = 53) and annual water discharge (R = 0.568, p < 0.0001, N = 53).

A direct quantification of the degree of preservation of the bedforms that have generated the studied cross-strata is offered by the ratio between preserved cross-set thickness and formative dune height (e.g. Leclair & Bridge, 2001; Jerolmack & Mohrig, 2005). This type of quantification is not applicable to individual cross-sets in this study, since the geometry of the formative bedform of each set is unknown. However, it is possible to make some inference on bedform preservation, at least in general terms, by considering the ratio between the average cross-set thickness and the average dune height. In some of the studied examples (N = 10), estimations of average dune height for bankfull conditions based on the empirical relationships by Bradley & Venditti (2017) are smaller than the corresponding mean thicknesses of the measured cross-sets (cf. Leclair, 2002). In principle, this is not necessarily unrealistic, because this quantity is a ratio of averages, not an average preservation ratio; these values could indicate that the cross-stratification produced by larger dunes is preferentially preserved (for example, because cross-strata may exclusively record flood conditions in thalweg areas) and that the bedforms are almost fully preserved. However, it is more likely that these results highlight errors in the estimations of formative dune geometry as a limitation of the approach. On average, the ratio between mean cross-set thickness and predicted mean dune height at bankfull is equal to 0.49 (standard deviation: 0.40, N = 53); a preservation ratio of *ca* 0.33 is generally expected for dune deposits based on theory and physical models (Leclair & Bridge, 2001; Leclair, 2002). Ratios between average cross-set thicknesses and average dune heights based on field data display negative correlations with log-transformed values of drainage-basin area (R = −0.649, p < 0.0001, N = 35) and mean annual discharge (R = −0.638, p < 0.0001, N = 35). This suggests that bedform preservation may be relatively reduced for larger rivers. As expected on the basis of the results reported above (Fig. 14), a negative relationship is also seen between $CV(d_{st})$ and the ratios between average cross-set thicknesses and average measured dune heights (R = −0.455, p = 0.0062, N = 35): increased bedform preservation appears to be associated with less variable cross-set thicknesses (cf. Leary & Ganti, 2020). Care must be taken in considering this particular result, however, since the mean cross-set thickness appears in both terms being correlated.

In the studied examples, two markedly seasonal ephemeral rivers that are prone to flashy floods (rivers Gash and Palar) are included. The deposits of these ephemeral rivers yield $CV(d_{st})$ values that are on average smaller (mean: 0.28, N = 4) than those of the perennial rivers (mean: 0.59, N = 49).

DISCUSSION

The use of $CV(D_{st})$ as discharge-variability proxy

The analysis presented here permits an assessment of the utility of the coefficient of variation of dune-scale cross-set thickness, $CV(D_{st})$, as an indicator of event-scale discharge variability in the way proposed by Leary & Ganti (2020). It is therefore a test of the applicability of $CV(D_{st})$ to palaeohydraulic and palaeohydrological reconstructions of the ancient stratigraphic record. The results presented herein do not fully support the proposed application of $CV(D_{st})$ as an indicator of flood-discharge peakedness relative to bedform turnover speed. It is recognized that dune-scale cross-sets returning the largest $CV(D_{st})$ values are associated with some of the longest flood recessions, and differences in the records of perennial rivers and ephemeral rivers subject to flash floods suggest that discharge variability may indeed affect cross-set thickness distribution. However, much of the remaining evidence does not support the use of $CV(D_{st})$ as a diagnostic tool for determining the peakedness of flood hydrographs. The principal finding is that groups of cross-sets with smaller

$CV(D_{st})$ values are not systematically associated with a rate of change in water discharge and bedform geometry and celerity that should favour bedform disequilibrium ($T^* < 1$), as proposed by Leary and Ganti (2020). These results warn of the danger of overinterpretation of the palaeohydrological significance of $CV(D_{st})$, and highlight the need to better constrain the mechanics underpinning bedform preservation and to identify the limits in the application of $CV(D_{st})$ to natural river systems. Sound process-to-product relationships based on experimental models may not always apply in an inverse product-to-process analysis because of the interference of multiple factors.

Potential causes of discrepancies from the model

The results do not provide a definitive explanation as to why the $CV(D_{st})$ of dune cross-strata would be a poor predictor of formative-bedform disequilibrium, but some possibilities can be explored.

Limitations in data and analyses

It is possible that the expected relationship between $CV(D_{st})$ and T^* is not observed because of limitations in the types of data used and analyses undertaken herein. Important limitations include: (i) the uncertainty on the representativeness to formative flow conditions of T_t and T_f values based on field data, especially for older deposits; (ii) potential error introduced by the application of empirical relationships such as those prescribing scaling between river size, bankfull flow conditions and dune geometry and kinematics; (iii) error introduced by the use of multiple data types and by heterogeneity in data dimensionality (1D versus 2D); (iv) systematic bias introduced through preferential sampling of restricted depositional niches and systems, such as the inclusion of only two ephemeral rivers; (v) the effect of thickness variability within each individual set of cross-stratification; and (vi) variability in the definition of samples for which the $CV(D_{st})$ values of the preserved sets are calculated, which commonly consist of groups of cosets, rather than individual cosets formed by single floods. The latter point is particularly important in consideration of the likelihood of compounding intra-coset and inter-coset variability in cross-strata thickness, and should be addressed in future studies through collection of purposely acquired data.

*Assumptions on floods and T**

Beside limitations of the data, including the fact that most T^* values represent average conditions for the studied rivers, some of the assumptions that underpin the hypothesis of Leary & Ganti (2020) may not be readily applicable in practice. The duration of flood recession is adopted as a simple measure of formative flows despite the intrinsically transient flow characteristics of flood events and possible changes from upper to lower flow regime conditions. Thus, it is possible that relative differences in T^* values – even when computed for the specific formative events of cross-strata rather than averaged to quantify overall river hydraulics – do not always capture bedform disequilibrium in an adequate manner. The thickness distributions analysed here represent the deposits of multiple floods, which may vary with respect to duration and peakedness. If preservation indeed varies as a function of the duration of flood recessions, there ought to be a vertical change in preservation through the preserved expression of a channel profile, because temporary flows over bar-tops are intrinsically short-lived, whereas thalweg regions of perennial rivers experience constant flows (Reesink *et al.,* 2015).

The theoretical framework of Leary & Ganti (2020) was developed based on the assumption that all preserved deposits are produced by floods; their flume experiments could not account for the potential occurrence of more localized, stage-dependent deposition on and around bars (cf. Bridge, 1993). Dune disequilibrium is known to vary vertically through a channel profile and horizontally across bars, in response to spatial variations in the flow field, and this is likely to change both within and between river channels (Reesink *et al.,* 2018). The sets analysed here come from different elevations within a channel, and thus encompass such variability in dune dynamics. This variability is explicitly acknowledged in the hierarchy hypothesis of Ganti *et al.* (2020) but is yet to be integrated with ideas about flow unsteadiness.

It can also be hypothesized that the frequency of flow recurrence will affect dune preservation because the flow field that shapes and deforms the dunes is controlled by inherited antecedent morphology. This type of morphodynamic feedback operates on multiple scales: at the scale of the dunes, and the overarching scale of the bars that define the hydraulic context. Relating general variability in set thickness in lithosomes to average measures of flood-hydrograph peakedness may not suit application to all rivers, and the applicability of the concept may well differ across different planforms that contrast in terms of specific local hydraulic conditions.

Additional controls on preservation

It is possible that other factors that affect the variability in the thickness of dune-scale cross-sets override any potential control by flood-discharge peakedness (Fig. 15). Several factors can potentially play a role in this, including: (i) dune and scour size distributions; and (ii) the influence of bedform hierarchy.

The migration of bedforms with variable depths of lee-side scour is commonly invoked as an autogenic mechanism determining the distribution of the thickness of cross-sets, as portrayed in the variability-dominated preservation model of Paola & Borgman (1991). Results presented herein can be contrasted with the expected variance in cross-set thickness that would arise from the theoretical 'variability-dominated' model of Paola & Borgman (1991), which posits that $CV(D_{st})$ values of *ca* 0.88 should be expected. About a quarter of the examples studied herein are characterized by $CV(D_{st})$ values in the 0.88 ± 0.3 range: the variability-dominated model, as specifically formalized by Paola & Borgman (1991), may account for these observations. The reported statistics refer to groups of sets that do not always represent cosets identified via the criteria outlined by Paola & Borgman (1991), but values of $CV(D_{st})$ that are consistently outside of the 0.88 ± 0.3 range have also been documented in cases where statistical analyses are applied to samples representing cosets, and have been interpreted to represent a record of prevalent bedform disequilibrium (Lyster *et al.* 2022).

It is possible that these results simply indicate that, in nature, the translation of dune topography generates sets that are usually less variable (in relative terms) than predicted by the variability-dominated preservation model of Paola & Borgman (1991), which may be conceptually sound but not formalized numerically in a way that is necessarily always realistic. It is recognized, for instance, that the assumed gamma-distributed dune relief may not be an accurate descriptor of natural dune topographies (Bridge, 1997; Leclair *et al.,* 1997). The specific probability density function employed to describe cross-set thickness distributions by Paola & Borgman (1991), which yields the expected 0.88 value of $CV(D_{st})$, relies on the fit of an exponential curve to the tail of the distribution of bedform heights, whereby both mean and standard deviation of cross-set thickness distributions are linear functions of the breadth of this tail. Even though this assumption has been found to be realistic in experimental settings under steady-state flow (Ganti *et al.,* 2013; Leary & Ganti, 2020), it is possible that this particular aspect of the model by Paola & Borgman (1991) is not universally applicable, due to its foundation on the premise of constant flow conditions. Thus, the relief variability in trains of dunes may still represent a primary mechanism of autogenic shredding (*sensu* Jerolmack & Paola, 2010) of any palaeohydraulic signal. Recent work has been devoted to analysis of additional controls on dune size and scour, such as transport stage (e.g. Das *et al.,* 2022), streambed material (e.g. Parsons *et al.,* 2016), and presence of horizons resistant to erosion, such as pavements (e.g. Tuijnder *et al.,* 2009): all of these factors may affect $CV(D_{st})$. The importance of these factors must be better constrained through future research efforts.

Sediment preservation and set thickness distributions may additionally be affected by the coupling of dunes with higher-scale geomorphic elements. Such bedform hierarchy changes local deposition rates, dune migration rates and bedform interactions, and therefore affects all underpinning assumptions of the 'variability-dominated' model (Reesink *et al.,* 2015; Paola *et al.,* 2018; Ganti *et al.,* 2020). Bedform hierarchy varies markedly between river systems, and is visibly expressed in the relative abundance of unit bars or in the variable degree of macroform development, for example. In addition to the effect of morphology on preservation, spatial variability in bathymetry can control variability in cross-set thickness distributions. For example, lateral variations in dune size along bar slopes may translate to vertical variations in set thickness. Where dune stability exists over a broader range of depths, such as in large rivers, increased variability in dune dimensions along bar slopes is expected. Notably, cross-sets developed at different levels along an accreting bar will also be characterized by variable preservation potential, which will be lowest at the bar top; sets produced by low-lying dunes, which are likely to be larger than average, may be preferentially preserved.

Systematic variations in dune topography and preservation with river size

A driver of sediment preservation that deserves particular attention is the relative magnitude of rates of dune migration and streambed aggradation or barform accretion (Bridge, 1997; Leclair, 2002;

Jerolmack & Mohrig, 2005). Larger rivers tend to be characterized by larger and finer-grained dunes, which tend to migrate more slowly for a given unit sediment flux compared to the smaller and coarser-grained dunes of smaller rivers (cf. Mahon & McElroy, 2018; Zomer *et al.,* 2021). This reflects two factors, primarily. Firstly, dune celerity should be inversely proportional to dune height, for a given rate of sediment transport (Exner 1920; Bagnold 1941; Simons *et al.* 1965). However, experimental data suggest that the effect of dune height on migration rates may be of limited importance (Leclair 2002). Secondly, dune celerity tends to increase with increasing streambed sediment grain size, possibly because of the greater drag force experienced by coarser grains and/or due to a relative decrease in sediment suspension (Nikora *et al.,* 1997; Lin & Venditti, 2013).

In parallel with inverse scaling between river size and dune celerity, direct proportionality between river scale and channel lateral migration rates is generally documented; such scaling between macroform migration (i.e. channel mobility) and river size reflects controls by sediment flux and water discharge, which tend to increase with river size (Hooke, 1980; Hudson & Kesel, 2000; Wickert *et al.,* 2013; Bufe *et al.,* 2019). Since channel migration rates determine the rate of accretion of macroforms (such as braid bars or point bars) and the rate of infill of major riverbed scours (for example, at channel-thread confluences), it may be expected that the ratio between local streambed accretion rate and bedform migration rate increases on average as a direct function of the scale of the river systems. It may therefore be expected that the preservation of cross-strata is higher on average for larger rivers with more rapidly shifting channels. In addition, larger, deeper rivers tend to exhibit more variable dune topographies (McElroy & Mohrig, 2009; Bradley & Venditti, 2017, their supplementary material; Myrow *et al.,* 2018), as do rivers with smaller T^* (Allen, 1976a), and this overall increase in topographic variability with river scale is thought to favour increased bedform preservation (Paola & Borgman, 1991). However, in the small number of cases in which estimations of average preservation could be determined, larger river systems tend to be characterized by more limited preservation, presumably because the increase in bedform size with river scale outpaces the increase in likelihood of bedform preservation due to morphodynamic hierarchy. Furthermore, an increase in barform accretion rate relative to bedform celerity is expected to result in a trend of decrease in $CV(D_{st})$ with river size (Jerolmack & Mohrig, 2005), but a tendency of increase in $CV(D_{st})$ with river-system scale is observed instead. As such, the observed relationships between river size, estimated bedform preservation and $CV(D_{st})$ challenge existing ideas on morphodynamic controls on dune-scale cross-strata. Further research is needed to discover why this may be the case.

On a representative sample of preserved dune deposits

The discussion above reveals that one of the key assumptions underpinning the application of both the variability-dominated model of Paola and Borgman (1991) and the unsteadiness hypothesis by Leary and Ganti (2020) is the notion of 'channel-scale interpretability'. In this study, like many others, the data are averaged vertically and horizontally. Implicit herein is the assumption that river channels can be interpreted as single entities for which a single distribution of dune cross-set thicknesses may be meaningful. This notion of channel-scale interpretability has embedded itself as a paradigm in the practice of interpreting fluvial deposits, possibly because it serves the aim of interpreting average river channel characteristics such as planform, depth, discharge and T^*.

However, sediment preservation is a selective and nonlinear filter (Jerolmack & Paola, 2010), and local conditions may significantly alter preservation potential within individual channels (Reesink *et al.,* 2015). It therefore follows that sediment preservation potential should vary within river channels, resulting in some unknown heterogeneity in dune-set preservation. It is at present not understood at what scale preserved dune sets need to be analysed and interpreted, or how preservation at a small scale and reflecting relatively short formative time spans can be upscaled to capture river behaviours over longer time periods. Attention must therefore be drawn to the need to define representative samples of dune sets that can be related to meaningful formative palaeohydraulic variables, by analogy with the concept of *'representative elementary volume'* that is used in hydrology and material sciences (Bachmat & Bear, 1987). A clear definition of a representative elementary volume of dune deposits would help to define optimal temporal and spatial scales for quantitative interpretations, help to address the challenge of upscaling, and highlight underpinning assumptions that require further research.

Additional considerations on rock-record interpretations

Perhaps, the most meaningful tests of the value of $CV(D_{st})$ for studies in palaeohydrology can be made by considering changes in $CV(D_{st})$ in time-resolved, ancient stratigraphic successions that are likely to record temporal changes in hydrological regime and flood-hydrograph characteristics. Some analysis of this type was undertaken by Leary & Ganti (2020), who considered data on cross-set thickness statistics from Palaeogene units of the Tremp Group of the Spanish Pyrenees, originally presented by Colombera *et al.* (2017), to interpret differences in stream discharge characteristic supposedly associated with climatic forcing during the Palaeocene–Eocene Thermal Maximum (PETM). However, the lower interval of the rock unit they considered as entirely syn-PETM (Claret Formation) actually pre-dates the beginning of the hyperthermal event. In reality, differences in $CV(D_{st})$ values of true pre-PETM and syn-PETM deposits within this specific unit (Claret Formation) are minimal, being 0.53 and 0.46, respectively. The more marked difference in $CV(D_{st})$ discussed by Leary & Ganti (2020) (0.69 versus 0.38) maps onto changes in facies and sedimentary architecture between the Esplugafreda and Claret formations, which have been interpreted in terms of an overall transition towards a less flashy discharge regime and more pronounced barform development (Colombera *et al.,* 2017; Arevalo *et al.,* 2022; cf. Basilici *et al.,* 2022). This interpretation is itself at odds with the supposed environmental significance of $CV(D_{st})$ envisaged by Leary & Ganti (2020). Additional research on ancient successions that preserve a record of temporal variations in flood behaviour is therefore still needed to elucidate the palaeohydrological significance of thickness distributions of cross-strata and, more generally, to assess the applicability of process-to-product models derived from controlled experiments to interpret the wide range of possible palaeohydrological controls that shaped the rock record.

CONCLUSIONS

Existing data on preserved dune-scale cross-set thicknesses from several rivers have been used to assess our ability to infer bedform disequilibrium and flood-discharge variability on the basis of the coefficient of variation of cross-set thickness, $CV(D_{st})$. As such, a test has been made of the predictive power of experimentally founded process-to-product models for product-to-process interpretations of ancient stratigraphy.

This study is affected by several limitations, including the combination of multiple data types and the limited representativeness of the considered river attributes to the specific formative conditions of the studied deposits. However, some general considerations can be made. Values of $CV(D_{st})$ in dune deposits tend to be well below 0.88 in many of the studied examples – an observation that may be interpreted to represent dominance of bedform-flow disequilibrium. Yet, $CV(D_{st})$ does not appear to vary in accord with T^* values computed to estimate the likelihood of disequilibrium in the studied river reaches, based on typical flood recession duration and inferred speed of bedform turnover. Also, larger rivers tend to be characterized by discharge and bedform characteristics that should favour, in relative terms, conditions of disequilibrium. However, these conditions are not matched with a systematic decrease in $CV(D_{st})$. A crucial observation is that the $CV(D_{st})$ of preserved channel deposits does not appear as a reliable proxy for the peakedness of the typical flood-hydrograph of the studied river reaches. Thus, results presented here caution against the use of $CV(D_{st})$ as a direct indicator of formative flow conditions.

It is possible that discrepancies from the model arise due to the interference of other factors. These discrepancies may be explained by differences between river systems in terms of distributions of dune size and scour, discharge variability, sediment types and transport stages, and preservation potential linked to bedform hierarchy. Approximately 25% of the preserved dune deposits in this study exhibit statistics that can be ascribed to variability in scour depths in trains of dunes, as formulated in the 'variability-dominated' preservation model. Differences in dune preservation can be further explained by differences between river systems, which may contrast with respect to distributions of dune size and scour depth, sediment types and sorting, transport stages, and preservation potential linked to bedform hierarchy. However, no single overriding control emerges from our analyses, suggesting that dune preservation may be variable within and between rivers, and that river channel deposits may exhibit an internal heterogeneity in dune preservation potential.

Overall, the coefficient of variation of dune-scale cross-set thickness, $CV(D_{st})$, appears to have limited value as a proxy for water-discharge variability on its own, but no other single overriding control on cross-set thickness variability emerges from our analyses. It is therefore recommended that future research is undertaken using improved constraints on formative conditions and considering a wider range of factors that may affect sediment preservation.

ACKNOWLEDGEMENTS

We thank the sponsors of the Fluvial, Eolian & Shallow-Marine Research Group at the University of Leeds for financial support to this research (AkerBP, Areva [now Orano], BHP, Cairn India [Vedanta], Chevron, CNOOC International, ConocoPhillips, Equinor, Murphy Oil, Occidental, Saudi Aramco, Shell, Tullow Oil, Woodside, and YPF). We thank Jan Alexander, John Holbrook, three anonymous reviewers and Associate Editor Chris Fielding for their constructive criticism, which has improved the article.

DATA AVAILABILITY STATEMENT

The data presented in the article are made available in the supplementary material (S2).

REFERENCES

Abdullatif, O. M. (1989). Channel-fill and sheet-flood facies sequences in the ephemeral terminal River Gash, Kassala, Sudan. *Sedimentary Geology*, **63**, 171-184.

Alexander, J., Bridge, J. S., Leeder, M. R., Collier, R. E. Ll., and **Gawthorpe, R. L.** (1994). Holocene meander-belt evolution in an active extensional basin, southwestern Montana. *Journal of Sedimentary Research*, **64**, 542-559.

Allen, J. R. L. (1973). Phase differences between bed configuration and flow in natural environments, and their geological relevance. *Sedimentology*, **20**, 323-329.

Allen, J. R. L. (1976a). Computational models for dune time-lag: Population structures and the effects of discharge pattern and coefficient of change. *Sedimentary Geology*, **16**, 99-130.

Allen, J. R. L. (1976b). Time-lag of dunes in unsteady flows: an analysis of Nasner's data from the R. Weser, Germany. *Sedimentary Geology*, **15**, 309-321.

Allen, J. R. L. and **Friend, P. F.** (1976). Relaxation time of dunes in decelerating aqueous flows. *Journal of the Geological Society*, **132**, 17-26.

Amsler, M. L. and **Garcia, M. H.** (1997). Sand-dune geometry of large rivers during floods – discussion. *Journal of Hydraulic Engineering*, **123**, 582-585.

Amsler, M. L., Prendes, H. H., Montagnini, M. D., Szupiany, R. and **Garcia, M. H.** (2003). Prediction of dune height in sand-bed rivers: The case of the Paraná River, Argentina. *Proceedings of the 3rd IAHR Symposium on River, Coastal and Estuarine Morphodynamics*, pp. 1104-1113, Madrid.

Andreadis, K. M., Schumann, G. J. P. and **Pavelsky, T.** (2013). A simple global river bankfull width and depth database. *Water Resources Research*, **49**, 7164-7168.

Arévalo, O. J., Colombera, L., Mountney, N. P., Basilici, G. and **Soares, M. V. T.** (2022). Variations in water discharge at different temporal scales in a mud-prone alluvial succession: The Paleocene-Eocene of the Tremp-Graus Basin, Spain. *Sedimentary Geology*, **433**, 106122.

Ashworth, P. J. and **Lewin, J.** (2012). How do big rivers come to be different?. *Earth-Science Reviews*, **114**, 84-107.

Ashworth, P. J., Sambrook Smith, G. H., Best, J. L., Bridge, J. S., Lane, S. N., Lunt, I. A., Reesink, A.J., Simpson, C.J. and **Thomas, R. E.** (2011). Evolution and sedimentology of a channel fill in the sandy braided South Saskatchewan River and its comparison to the deposits of an adjacent compound bar. *Sedimentology*, **58**, 1860-1883.

Ashida, K. and **Michiue, M.** (1973). Studies on bed-load transport rate in open channel flows. *Proceedings of the International Association for Hydraulic Research International Symposium on River Mechanics, 9-12 January 1973, Bangkok, Thailand*, pp. 407-417, Asian Institute of Technology, Bangkok.

Bachmat, Y. and **Bear, J.** (1987). On the concept and size of a representative elementary volume (REV). In: Advances in transport phenomena in porous media (Eds. Bear, J. and Corapcioglu, M. Y.), pp. 3-20, Springer, Dordrecht.

Bagnold, R. A. (1941). The physics of blown sand and desert dunes. Morrow, New York.

Barrell, J. (1917). Rhythms and the measurements of geologic time. *Bulletin of the Geological Society of America*, **28**, 745-904.

Basilici, G., Colombera, L., Soares, M. V. T., Arévalo, O. J., Mountney, N. P., Lorenzoni, P., de Souza Filho, C. R., Mesquita, Á. F. and **Janočko, J.** (2022). Variations from dry to aquic conditions in Vertisols (Esplugafreda Formation, Eastern Pyrenees, Spain): Implications for late Paleocene climate change. *Palaeogeography, Palaeoclimatology, Palaeoecology*, **595**, 110972.

Best, J. L., Ashworth, P. J., Bristow, C. S. and **Roden, J.** (2003). Three-dimensional sedimentary architecture of a large, mid-channel sand braid bar, Jamuna River, Bangladesh. *Journal of Sedimentary Research*, **73**, 516-530.

Best, J. L., Ashworth, P. J., Sarker, M. H. and **Roden, J. E.** (2007). The Brahmaputra-Jamuna River, Bangladesh. In: Large rivers: geomorphology and management (Ed. Gupta, A.), Wiley, Chichester, pp. 395-430.

Bradley, R. W. and **Venditti, J. G.** (2017). Reevaluating dune scaling relations. *Earth-Science Reviews*, **165**, 356-376.

Bradley, R. W. and **Venditti, J. G.** (2021). Mechanisms of dune growth and decay in rivers. *Geophysical Research Letters*, **48**, e2021GL094572.

Bridge, J. S. (1993). The interaction between channel geometry, water flow, sediment transport and deposition in braided rivers. In: *Braided Rivers* (Eds. Best, J.L., Bristow, C.S.), *Geological Society of London, Special Publication* 75, pp. 13-71.

Bridge, J. S. (1997). Thickness of sets of cross strata and planar strata as a function of formative bed-wave geometry and migration, and aggradation rate. *Geology*, **25**, 971-974.

Bridge, J. S. (2006). Fluvial facies models: recent developments. In: *Facies Models Revisited* (Eds. Posamentier, H., Walker, R.G.), *SEPM Special Publication* 84, pp. 85-170.

Bridge, J. S., Smith, N. D., Trent, F., Gabel, S. L. and **Bernstein, P.** (1986). Sedimentology and morphology of a low-sinuosity river: Calamus River, Nebraska Sand Hills. *Sedimentology*, **33**, 851-870.

Bridge, J. S., Alexander, J. A. N., Collier, R. E. Ll., Gawthorpe, R. L. and **Jarvis, J.** (1995). Ground-penetrating radar and coring used to study the large-scale structure of point-bar deposits in three dimensions. *Sedimentology*, **42**, 839-852.

Bristow, C. S. (1993). Sedimentary structures exposed in bar tops in the Brahmaputra River, Bangladesh. In: *Braided Rivers* (Eds. Best, J.L., Bristow, C.S.), *Geological Society of London, Special Publication* 75, pp. 277-289.

Bufe, A., Turowski, J. M., Burbank, D. W., Paola, C., Wickert, A. D. and **Tofelde, S.** (2019). Controls on the lateral channel-migration rate of braided channel systems in coarse non-cohesive sediment. *Earth Surface Processes and Landforms*, **44**, 2823-2836.

Chorley, R. J. (1969). The drainage basin as the fundamental geomorphic unit. In: (Ed. Chorley, R. J..), Water, earth, and man: a synthesis of hydrology, geomorphology and socio-economic geography, pp. 77-99, Methuen, London.

Chung, G. S., Lee, J. Y., Yang, D. Y. and Kim, **J. Y.** (2005). Architectural Elements of the Fluvial Deposits of Meander Bends in Midstream of the Yeongsan River, Korea. *Journal of the Korean Earth Science Society*, **26**, 809-820.

Claude, N., Rodrigues, S., Bustillo, V., Bréhéret, J. G., Macaire, J. J. and **Jugé, P.** (2012). Estimating bedload transport in a large sand–gravel bed river from direct sampling, dune tracking and empirical formulas. *Geomorphology*, **179**, 40-57.

Coleman, J. M. (1969). Brahmaputra River: channel processes and sedimentation. *Sedimentary Geology*, **3**, 129-239.

Collinson, J. D. (1970). Bedforms of the Tana river, Norway. *Geografiska Annaler: Series A, Physical Geography*, **52**, 31-56.

Colombera, L., Mountney, N. P. and **McCaffrey, W. D.** (2013). A quantitative approach to fluvial facies models: Methods and example results. *Sedimentology*, **60**, 1526-1558.

Colombera, L., Arévalo, O. J. and **Mountney, N. P.** (2017). Fluvial-system response to climate change: the Paleocene-Eocene Tremp group, Pyrenees, Spain. *Global and Planetary Change*, **157**, 1-17.

Crowley, K. D. (1983). Large-scale bed configurations (macroforms), Platte River Basin, Colorado and Nebraska: primary structures and formative processes. *Geological Society of America Bulletin*, **94**, 117-133.

Czapiga, M. J., McElroy, B. and **Parker, G.** (2019). Bankfull Shields number versus slope and grain size. *Journal of Hydraulic Research*, **57**, 760-769.

Das D., Ganti V., Bradley R., Venditti J., Reesink A. J. H. and **Parsons, D.** (2022) The influence of transport stage on preserved fluvial strata. *Geophysical Research Letters*, e2022GL099808.

Davie, T. and **Quinn, N. W.** (2019). Fundamentals of hydrology, 3rd edition. Routledge, New York.

Eilertsen, R. S. and **Corner, G. D.** (2011). Role of scouring and base-level change in producing anomalously thick fluvial successions: an example from the Tana River, northern Norway. In: *From river to rock record: the preservation of fluvial sediments and their subsequent interpretation* (Eds. Davidson, S. K., Leleu, S. and North, C. P.), *SEPM Special Publication* 97, pp. 265-280.

Engelund, F. and **Fredsøe, J.** (1976). A sediment transport model for straight alluvial channels. *Hydrology Research*, **7**, 293-306.

Engelund, F. and **Hansen, E.** (1967). A monograph on sediment transport in alluvial streams. Technical University of Denmark, Copenhagen.

Exner, F. M. (1920). Zur physik der dünen. *Sitzungs Berichte Akademie des Wissenschaften*, **129**, 929–952.

Fielding, C. R., Alexander, J. and **Allen, J. P.** (2018). The role of discharge variability in the formation and preservation of alluvial sediment bodies. *Sedimentary Geology*, **365**, 1-20.

Frazier, D. E. and **Osanik, A.** (1961). Point-bar deposits, Old River Locksite, Louisiana. *Transactions of the Gulf Coast Association of Geological Societies*, **11**, 121-137.

Gabel, S. L. (1993). Geometry and kinematics of dunes during steady and unsteady flows in the Calamus River, Nebraska, USA. *Sedimentology*, **40**, 237-269.

Ganti, V., Paola, C. and **Foufoula-Georgiou, E.** (2013). Kinematic controls on the geometry of the preserved cross sets. *Journal of Geophysical Research: Earth Surface*, **118**, 1296-1307.

Ganti, V., Hajek, E. A., Leary, K., Straub, K. M. and **Paola, C.** (2020). Morphodynamic hierarchy and the fabric of the sedimentary record. *Geophysical Research Letters*, **47**, e2020GL087921.

Ghinassi, M. and **Moody, J.** (2021). Reconstruction of an extreme flood hydrograph and morphodynamics of a meander bend in a high-peak discharge variability river (Powder River, USA). *Sedimentology*, **68**, 3549-3576.

Gilluly, J. (1969). Geological perspective and the completeness of the geologic record. *Geological Society of America Bulletin*, **80**, 2303-2312.

Hackney, C. R., Darby, S. E., Parsons, D. R., Leyland, J., Aalto, R., Nicholas, A. P. and **Best, J. L.** (2018). The influence of flow discharge variations on the morphodynamics of a diffluence–confluence unit on a large river. *Earth Surface Processes and Landforms*, **43**, 349-362.

Hartley, A. J. and **Owen, A.** (2022). Paleohydraulic analysis of an ancient distributive fluvial system. *Journal of Sedimentary Research*, **92**, 445-459.

Herbert, C. M., Alexander, J., Amos, K. J. and **Fielding, C. R.** (2020). Unit bar architecture in a highly-variable fluvial discharge regime: Examples from the Burdekin River, Australia. *Sedimentology*, **67**, 576-605.

Hesselink, A. W., Weerts, H. J. and **Berendsen, H. J.** (2003). Alluvial architecture of the human-influenced river Rhine, The Netherlands. *Sedimentary Geology*, **161**, 229-248.

Hooke, J. M. (1980). Magnitude and distribution of rates of river bank erosion. *Earth Surface Processes*, **5**, 143-157.

Horn, J. D., Fielding, C. R. and **Joeckel, R. M.** (2012). Revision of Platte River alluvial facies model through observations of extant channels and barforms, and subsurface alluvial valley fills. *Journal of Sedimentary Research*, **82**, 72-91.

Hudson, P. F. and **Kesel, R. H.** (2000). Channel migration and meander-bend curvature in the lower Mississippi River prior to major human modification. *Geology*, **28**, 531-534.

Jerolmack, D. J. and **Mohrig, D.** (2005). Frozen dynamics of migrating bedforms. *Geology*, **33**(1), 57-60.

Jerolmack, D. J. and **Paola, C.** (2010). Shredding of environmental signals by sediment transport. *Geophysical Research Letters*, **37**, L19401.

Jones, C. M. (1977). Effects of varying discharge regimes on bed-form sedimentary structures in modern rivers. *Geology*, **5**, 567-570.

Jordan, D. W. and **Pryor, W. A.** (1992). Hierarchical levels of heterogeneity in a Mississippi River meander belt and application to reservoir systems. *AAPG Bulletin*, **76**, 1601-1624.

Julien, P. Y. (1992). Study of bedform geometry in large rivers. Delft Hydraulics Report Q1386, Delft.

Julien, P. Y., Klaassen, G. J., Ten Brinke, W. B. M. and **Wilbers, A. W. E.** (2002). Case study: bed resistance of Rhine River during 1998 flood. *Journal of Hydraulic Engineering*, **128**, 1042-1050.

Kleinhans, M. G. (2001). The key role of fluvial dunes in transport and deposition of sand–gravel mixtures, a preliminary note. *Sedimentary Geology*, **143**, 7-13.

Kleinhans, M. G. (2002). Sorting out sand and gravel: sediment transport and deposition in sand-gravel bed rivers. PhD Thesis, University of Utrecht, The Netherlands.

Kleinhans, M. G. and **Ten Brinke, W. B.** (2001). Accuracy of cross-channel sampled sediment transport in large sand-gravel-bed rivers. *Journal of Hydraulic Engineering*, **127**, 258-269.

Kolmogorov, A. N. (1951). Solution of a problem in probability theory connected with the problem of the mechanism of stratification. *Transactions of the American Mathematical Society*, **53**, 171-177.

Lajeunesse, E., Malverti, L. and **Charru, F.** (2010). Bed load transport in turbulent flow at the grain scale: Experiments and modeling. *Journal of Geophysical Research: Earth Surface*, **115**(F4), F04001.

Leary, K. C. and **Ganti, V.** (2020). Preserved fluvial cross strata record bedform disequilibrium dynamics. *Geophysical Research Letters*, **47**, e2019GL085910.

Leclair, S. F. (2002). Preservation of cross-strata due to the migration of subaqueous dunes: an experimental investigation. *Sedimentology*, **49**, 1157-1180.

Leclair, S. F. (2006). New pieces to the puzzle of reconstructing sediment paleofluxes from river dune deposits. *Geology*, **34**, 401-404.

Leclair, S. F. and **Bridge, J. S.** (2001). Quantitative interpretation of sedimentary structures formed by river dunes. *Journal of Sedimentary Research*, **71**, 713-716.

Leclair, S. F., Bridge, J. S. and **Wang, F.** (1997). Preservation of cross-strata due to migration of subaqueous dunes over aggrading and non-aggrading beds: comparison of experimental data with theory. *Geoscience Canada*, **24**, 55-66.

Leier, A. L., DeCelles, P. G. and **Pelletier, J. D.** (2005). Mountains, monsoons, and megafans. *Geology*, **33**, 289-292.

Lin, C.-Y. M. and **Venditti, J. G.** (2013). An empirical model of subcritical bedform migration. *Sedimentology*, **60**, 1786-1799.

Lisimenka, A., Kubicki, A. and **Kałas, M.** (2022). Bedforms evolution in the Vistula River mouth during extreme flood event, southern Baltic Sea. *Oceanologia*, **64**, 212-226.

Lotsari, E., Veijalainen, N., Alho, P. and **Käyhkö, J.** (2010). Impact of climate change on future discharges and flow characteristics of the Tana River, sub-arctic northern Fennoscandia. *Geografiska Annaler: Series A, Physical Geography*, **92**, 263-284.

Lunt, I. A., Sambrook Smith, G. H., Best, J. L., Ashworth, P. J., Lane, S. N. and **Simpson, C. J.** (2013). Deposits of the sandy braided South Saskatchewan River: Implications for the use of modern analogs in reconstructing channel dimensions in reservoir characterization. *AAPG Bulletin*, **97**, 553-576.

Lyster, S. J., Whittaker, A. C., Hajek, E. A. and **Ganti, V.** (2022). Field evidence for disequilibrium dynamics in preserved fluvial cross-strata: A record of discharge variability or morphodynamic hierarchy?. *Earth and Planetary Science Letters*, **579**, 117355.

Mahon, R. C. and **McElroy, B.** (2018). Indirect estimation of bedload flux from modern sand-bed rivers and ancient fluvial strata. *Geology*, **46**, 579-582.

Martin, R. L. and **Jerolmack, D. J.** (2013). Origin of hysteresis in bed form response to unsteady flows. *Water Resources Research*, **49**, 1314-1333.

McElroy, B. and **Mohrig, D.** (2009). Nature of deformation of sandy bed forms. *Journal of Geophysical Research: Earth Surface*, **114**, F00A04.

McLeod, J. S., Wood, J., Lyster, S. J., Valenza, J. M., Spencer, A. R. and **Whittaker, A. C.** (2023). Quantitative constraints on flood variability in the rock record. *Nature Communications*, **14**, 3362.

Meyer-Peter, E. and **Müller, R.** (1948). Formulas for bed-load transport. *Proceedings of the 2nd Meeting of the International Association for Hydraulic Structures Research*, pp. 39-64, IAHR, Stockholm.

Miall, A. D. (1985). Architectural-element analysis: a new method of facies analysis applied to fluvial deposits. *Earth-Science Reviews*, **22**, 261-308.

Moody, J. A. and **Troutman, B. M.** (2002). Characterization of the spatial variability of channel morphology. *Earth Surface Processes and Landforms*, **27**, 1251-1266.

Myrow, P. M., Jerolmack, D. J. and **Perron, J. T.** (2018). Bedform disequilibrium. *Journal of Sedimentary Research*, **88**, 1096-1113.

Naqshband, S., Hurther, D., Giri, S., Bradley, R. W., Kostaschuk, R. A., Venditti, J. G. and **Hoitink, A. J. F.** (2021). The influence of slipface angle on fluvial dune growth. *Journal of Geophysical Research: Earth Surface*, **126**, e2020JF005959.

Nikora, V. I., Sukhodolov, A. N. and **Rowinski, P. M.** (1997). Statistical sand wave dynamics in one-directional water flows. *Journal of Fluid Mechanics*, **351**, 17-39.

Paarlberg, A. J., Dohmen-Janssen, C. M., Hulscher, S. J., Termes, P. and **Schielen, R.** (2010). Modelling the effect of time-dependent river dune evolution on bed roughness and stage. *Earth Surface Processes and Landforms*, **35**, 1854-1866.

Paola, C. and **Borgman, L.** (1991). Reconstructing random topography from preserved stratification. *Sedimentology*, **38**, 553-565.

Parker, N. O. (2010). Distinguishing flood frequency and magnitude in the morphodynamics and sedimentology of rivers: insights from the South Saskatchewan River, Canada. PhD Thesis, University of Birmingham.

Parsons, D. R., Best, J. L., Orfeo, O., Hardy, R. J., Kostaschuk, R. and **Lane, S. N.** (2005). Morphology and flow fields of three-dimensional dunes, Rio Paraná, Argentina: Results from simultaneous multibeam echo sounding and acoustic Doppler current profiling. *Journal of Geophysical Research: Earth Surface*, **110**, 2004JF000231.

Parsons, D. R., Schindler, R. J., Hope, J. A., Malarkey, J., Baas, J. H., Peakall, J., Manning, A.J., Ye, L., Simmons, S., Paterson, D. M., Aspden, R. J., Bass, S. J., Davies, A. G., Lichtman, I. D. and **Thorne, P. D.** (2016). The role of biophysical cohesion on subaqueous bed form size. *Geophysical Research Letters*, **43**, 1566-1573.

Reesink, A. J., Ashworth, P. J., Sambrook Smith, G. H., Best, J. L., Parsons, D. R., Amsler, M. L., Hardy, R.J., Lane, S.N., Nicholas, A.P., Orfeo, O., Sandbach, S.D., Simpson, C. J. and **Szupiany, R. N.** (2014). Scales and causes of heterogeneity in bars in a large multi-channel river: Río Paraná, Argentina. *Sedimentology*, **61**, 1055-1085.

Reesink, A. J. H., Van den Berg, J. H., Parsons, D. R., Amsler, M. L., Best, J. L., Hardy, R. J., Orfeo, O. and **Szupiany, R. N.** (2015). Extremes in dune preservation: Controls on the completeness of fluvial deposits. *Earth-Science Reviews*, **150**, 652-665.

Reesink, A. J. H., Parsons, D. R., Ashworth, P. J., Best, J. L., Hardy, R. J., Murphy, B. J., McLelland, S.J. and **Unsworth, C.** (2018). The adaptation of dunes to changes in river flow. *Earth-Science Reviews*, **185**, 1065-1087.

Resmi, M. R. and **Achyuthan, H.** (2018). Northeast monsoon variations during the Holocene inferred from palaeochannels and active channels of the Palar River basin, Southern Peninsular India. *The Holocene*, **28**, 895-913.

Resmi, M. R., Achyuthan, H. and **Jaiswal, M. K.** (2017). Middle to late Holocene paleochannels and migration of the Palar River, Tamil Nadu: Implications of neotectonic activity. *Quaternary International*, **443**, 211-222.

Resmi, M. R., Achyuthan, H. and **Babeesh, C.** (2021). Holocene evolution of the Palar river, Southern India: Tracking history of migration, provenance, weathering and tectonics. *Quaternary İnternational*, **575**, 358-374.

Rodrigues, S., Mosselman, E., Claude, N., Wintenberger, C. L. and **Juge, P.** (2015). Alternate bars in a sandy gravel bed river: generation, migration and interactions with superimposed dunes. *Earth Surface Processes and Landforms*, **40**, 610-628.

Rubin, D. M. and **Hunter, R. E.** (1982). Bedform climbing in theory and nature. *Sedimentology*, **29**, 121-138.

Sambrook Smith, G. H., Ashworth, P. J., Best, J. L., Lunt, I. A., Orfeo, O. and **Parsons, D. R.** (2009). The sedimentology and alluvial architecture of a large braid bar, Río Paraná, Argentina. *Journal of Sedimentary Research*, **79**, 629-642.

Sambrook Smith, G. H., Best, J. L., Orfeo, O., Vardy, M. E. and **Zinger, J. A.** (2013). Decimeter-scale in situ mapping of modern cross-bedded dune deposits using parametric echo sounding: A new method for linking river processes and their deposits. *Geophysical Research Letters*, **40**, 3883-3887.

Santos, M. L. D. and **Stevaux, J. C.** (2000). Facies and architectural analysis of channel sandy macroforms in the upper Parana river. *Quaternary International*, **72**, 87-94.

Serinaldi, F., Loecker, F., Kilsby, C. G. and **Bast, H.** (2018). Flood propagation and duration in large river basins: a data-driven analysis for reinsurance purposes. *Natural Hazards*, **94**, 71-92.

Shan, X., Shi, X., Clift, P. D., Seddique, A. A., Liu, S., Tan, C., Liu, J., Hasan, R., Li, J. and **Song, Z.** (2021). Sedimentology of the modern seasonal lower Ganges River with low inter-annual peak discharge variance, Bangladesh. *Journal of the Geological Society*, **178**, jgs2020-094.

Simons, D. B., Richardson, E. V. and **Nordin, C. F.** (1965). Bedload equation for ripples and dunes. Geological Survey Professional Paper 462-H, US Government Printing Office.

Singh, H., Parkash, B. and **Gohain, K.** (1993). Facies analysis of the Kosi megafan deposits. *Sedimentary Geology*, **85**, 87-113.

Smith, N. D. (1974). Sedimentology and bar formation in the upper Kicking Horse River, a braided outwash stream. *The Journal of Geology*, **82**, 205-223.

Strick, R. J., Ashworth, P. J., Sambrook Smith, G. H., Nicholas, A. P., Best, J. L., Lane, S. N., Parsons, D.R., Simpson, C.J., Unsworth, C.A. and **Dale, J.** (2019). Quantification of bedform dynamics and bedload sediment flux in sandy braided rivers from airborne and satellite imagery. *Earth Surface Processes and Landforms*, **44**, 953-972.

Sorby, H. C. (1859). On the structures produced by the currents present during the deposition of stratified rocks. *The Geologist*, **2**, 137-147.

Szupiany, R. N., Amsler, M. L., Hernandez, J., Parsons, D. R., Best, J. L., Fornari, E. and **Trento, A.** (2012). Flow fields, bed shear stresses, and suspended bed sediment dynamics in bifurcations of a large river. *Water Resources Research*, **48**, W11515.

Tuijnder, A. P., Ribberink, J. S. and **Hulscher, S. J.** (2009). An experimental study into the geometry of supply-limited dunes. *Sedimentology*, **56**, 1713-1727.

Unsworth, C. A., Parsons, D. R., Hardy, R. J., Reesink, A. J. H., Best, J. L., Ashworth, P. J. and **Keevil, G. M.** (2018). The impact of nonequilibrium flow on the structure of turbulence over river dunes. *Water Resources Research*, **54**, 6566-6584.

Wang, R., Colombera, L. and **Mountney, N. P.** (2020). Palaeohydrological characteristics and palaeogeographic reconstructions of incised-valley-fill systems: Insights from the Namurian successions of the United Kingdom and Ireland. *Sedimentology*, **67**, 3844-3873.

Wickert, A. D., Martin, J. M., Tal, M., Kim, W., Sheets, B. and **Paola, C.** (2013). River channel lateral mobility: Metrics, time scales, and controls. *Journal of Geophysical Research: Earth Surface*, **118**, 396-412.

Wilbers, A. W. E. (2004). The development and hydraulic roughness of subaqueous dunes. PhD Thesis, Utrecht University.

Wilbers, A. W. E. and **Ten Brinke, W. B. M.** (2003). The response of subaqueous dunes to floods in sand and gravel bed reaches of the Dutch Rhine. *Sedimentology*, **50**, 1013-1034.

Wintenberger, C. L., Rodrigues, S., Claude, N., Jugé, P., Bréhéret, J. G. and **Villar, M.** (2015). Dynamics of nonmigrating mid-channel bar and superimposed dunes in a sandy-gravelly river (Loire River, France). *Geomorphology*, **248**, 185-204.

Wright, S. and **Parker, G.** (2004). Flow resistance and suspended load in sand-bed rivers: simplified stratification model. *Journal of Hydraulic Engineering*, **130**, 796-805.

Zomer, J. Y., Naqshband, S., Vermeulen, B. and **Hoitink, A. J. F.** (2021). Rapidly migrating secondary bedforms can persist on the lee of slowly migrating primary river dunes. *Journal of Geophysical Research: Earth Surface*, **126**, e2020JF005918.

TABLE AND FIGURE CAPTIONS

Table 1: Summary of case studies, including data sources, data types and number of measured cross-set thicknesses (N). The number of observations is reported as grouped by case study, not by sample river reach. PES = parametric echo sounder.

Table 2: Results of correlation analyses for log-transformed values of $CV(D_{st})$ and T*. N = number of observations; R = Pearson's correlation coefficient; p = p-value.

Figure 1: Alluvial dunes and cross-strata. (A) and (B) Streamwise and lateral variability in dune geometry in the Mississippi (Louisiana); topobathymetric digital elevation model from the CoNED dataset (USGS). (C) Stack of sets of cross-stratified sandstone from the Lower Jurassic Kayenta Formation (south-east Utah).

Figure 2: Selected controls on dune and cross-strata geometries. (A) Effect of variable scour depths along a train of dune on the thickness distribution of the preserved cross-sets (Reesink *et al.,* 2015). (B) Bedform hysteresis expressed as changes in bedform geometry as a function of variations in average flow velocity $\overline{U}$ through time; time is shown on a logarithmic scale (Myrow *et al.,* 2018). (C) Evolution of average bedform heights versus water discharge for slow (left) and fast (right) flood waves (Martin & Jerolmack, 2013).

Figure 3: Illustration of quantifications of the thickness of a single set of dune-scale trough cross-stratification in one-dimensional (1D) and two-dimensional (2D) datasets, and of how these thickness measurements compare to the true maximum thickness of the cross-set. See Table 1 for list of 1D and 2D datasets.

Figure 4: Overall thickness distributions of sets of cross-strata recognized in 1D and 2D datasets (see Table 1); boxes represent interquartile ranges, horizontal bars inside the boxes represent median values, crosses (x) represent mean value, violin plots represent kernel densities.

Figure 5: Histograms and cumulative distribution functions of cross-set thickness of case studies for which the thickness of individual cross-strata is known (see Table 1).

Figure 6: Relationships between mean values of cross-set thickness in the studied river reaches and hydrological characteristics, including: (A) size of river catchment area; (B) mean yearly water discharge; and (C) discharge seasonality ('discharge peakedness' of Leier *et al.*, 2005; i.e. ratio between average discharge of wettest month and mean annual discharge). Corresponding data on 75th and 90th centiles of cross-set thickness distributions are included in Supplementary Fig. S1.

Figure 7: Comparison between observed dune morphometry and dune geometries predicted for bankfull conditions by application of the relationships by Bradley & Venditti (2017): (A) predicted versus observed dune heights; (B) predicted versus observed dune wavelengths.

Figure 8: Comparison of values of bedform turnover timescales (T_t) estimated based on values of bedform celerity inferred from channel slope (cf. Mahon & McElroy, 2018), in abscissa, and sediment flux (cf. Myrow *et al.,* 2018), in ordinate. The error bars indicate the range of T_t values associated with the range of calculated values of unit sediment flux.

Figure 9: Comparison between values of bedform turnover timescales (T_t) estimated based on field observations of dune morphometry and celerity, and corresponding values estimated based on dune celerity predicted using (A) channel slope (cf. Mahon & McElroy, 2018) and (B) sediment flux (cf. Myrow *et al.,* 2018). The bars in part B indicate the range of T_t values associated with the range of calculated values of unit sediment flux.

Figure 10: Comparison between values of flood-recession timescales (T_f) and values of bedform turnover timescales (T_t) estimated based on (A) channel gradient (cf. Mahon & McElroy, 2018) and (B) sediment flux (cf. Myrow *et al.,* 2018). Error bars indicate two standard deviations of T_f values. Spots are colour-coded by river catchment size.

Figure 11: Comparison between values of dune equilibrium numbers (T^*) reflecting bedform turnover timescales that are estimated using field observations of dune morphometry and celerity, and corresponding T^* values estimated based on dune celerity predicted from: (A) channel slope (cf. Mahon & McElroy, 2018); (B) sediment flux (cf. Myrow *et al.,* 2018); or (C) as reported by Leary &

Ganti (2020) for the same rivers. Spots are colour-coded by river catchment size, and scaled in size to mean annual discharge.

Figure 12: Scatterplots illustrating relationships between the coefficients of variation (CV) of cross-set thickness and values of bedform turnover timescales (T_t) estimated based on: (A) dune celerity predicted from channel slope (cf. Mahon & McElroy, 2018); (B) dune celerity predicted from sediment flux (cf. Myrow *et al.,* 2018); and (C) observations of dune morphometry and celerity. Spots are colour-coded by type of observation (see Table 1).

Figure 13: Scatterplot illustrating the relationship between the coefficients of variation (CV) of cross-set thickness and values of average flood-recession timescale (T_f). Spots are colour-coded by type of observation (see Table 1).

Figure 14: Scatterplots showing the relationships between the coefficients of variation (CV) of cross-set thickness of the studied reaches and values of dune equilibrium numbers (T*) reflecting bedform turnover timescales that are estimated based on: (A) dune celerity predicted from channel slope (cf. Mahon & McElroy, 2018); (B) dune celerity predicted from sediment flux (cf. Myrow *et al.,* 2018); (C) using field observations of dune morphometry and celerity; or (D) as reported by Leary & Ganti (2020) for the same rivers. Spots are colour-coded by river catchment size, and scaled in size to mean annual discharge.

Figure 15: Conceptual summary of selected controls on cross-set thickness statistics discussed in the text, and of their relationships with river-system size.

Table 2: Summary of case studies, including data sources, data types and number of measured cross-set thicknesses (N). The number of observations is reported as grouped by case study, not by sample river reach. PES = parametric echo sounder.

River	Source	Observation type	N	Bedform geometry data	Bedform celerity data
Brahmaputra	Best *et al.* (2003)	1D (core)	51	Julien (1992); Best *et al.* (2003, 2007)	Coleman (1969)
Brahmaputra	Bristow (1993)	2D (outcrop)	186	Julien (1992); Best *et al.* (2003, 2007)	Coleman (1969)
Burdekin	Herbert *et al.* (2020)	2D (trench)	90	N/A	N/A
Calamus	Bridge *et al.* (1986)	1D (core)	209	Gabel (1993)	Gabel (1993)
Ganges	Shan *et al.* (2020)	2D (outcrop)	32	N/A	N/A
Gash	Abdullatif (1989)	2D (outcrop, trench)	35	N/A	N/A
Kosi	Singh *et al.* (1993)	2D (outcrop, trench)	209	N/A	N/A
Loire	Leclair (2006); Leclair *et al.* (2011)	2D (outcrop)	50	Wintenberger *et al.* (2015)	Claude (2012)
Madison	Alexander *et al.* (1994)	1D (core)	12	N/A	N/A
Mississippi	Frazier & Osanik (1961)	2D (trench)	45	Frazier & Osanik (1961)	Frazier & Osanik (1961)
Mississippi	Jordan & Pryor (1992)	1D (core)	78	Jordan & Pryor (1992)	Jordan & Pryor (1992)
Palar	Resmi *et al.* (2017, 2021); Resmi & Achyuthan (2018)	1D (outcrop)	38	N/A	N/A
Paraná	Reesink *et al.* (2014)	1D (core)	116	Julien (1992); Amsler *et al.* (2003), Parsons *et al.* (2005); Ashworth & Lewin (2012); Szupiany *et al.* (2012)	Santos & Steveaux (2000); Parsons *et al.* (2005); Sambrook Smith *et al.* (2009)
Paraná	Sambrook Smith *et al.* (2013)	2D (PES)	822	Sambrook Smith *et al.* (2013)	Santos & Steveaux (2000); Parsons *et al.* (2005); Sambrook Smith *et al.* (2009)
Platte	Horn *et al.* (2012)	2D (trench)	74	Crowley (1983)	N/A
Powder River	Ghinassi & Moody (2021)	2D (trench)	101	N/A	N/A
South Esk	Bridge *et al.* (1995)	1D (core)	29	N/A	N/A
South Fork	Alexander *et al.* (1994)	1D (core)	103	N/A	N/A
South Saskatchewan	Ashworth *et al.* (2011); Lunt *et al.* (2013); Parker (2010)	1D (core)	276	Lunt *et al.* (2013)	Strick *et al.* (2019)
Tana	Eilertsen & Corner (2010)	2D (outcrop)	-	Collinson (1970)	N/A
Waal	Hesselink *et al.* (2003)	1D (core)	84	Wilbers (2004)	Kleinhans & Ten Brinke (2001)
Yeongsan	Chung *et al.* (2005)	1D (outcrop)	17	N/A	N/A

Table 2: Results of correlation analyses for log-transformed values of *CV(Dst)* and *T**. N = number of observations; R = Pearson's correlation coefficient; p = p-value.

***T** estimation**	**Dataset type**	**N**	**R**	**p**
Based on estimated channel slope	Any	53	−0.500497691	0.000138
	1D	33	−0.526754341	0.001667
	2D	20	0.080319525	0.736469
Based on estimated unit sediment flux	Any	53	−0.37158957	0.006241
	1D	33	−0.36644076	0.036194
	2D	20	−0.212310745	0.369555
Based on dune measurements	Any	30	−0.589304402	0.000616
	1D	23	−0.678760326	0.000378
	2D	7	0.11603723	0.804395

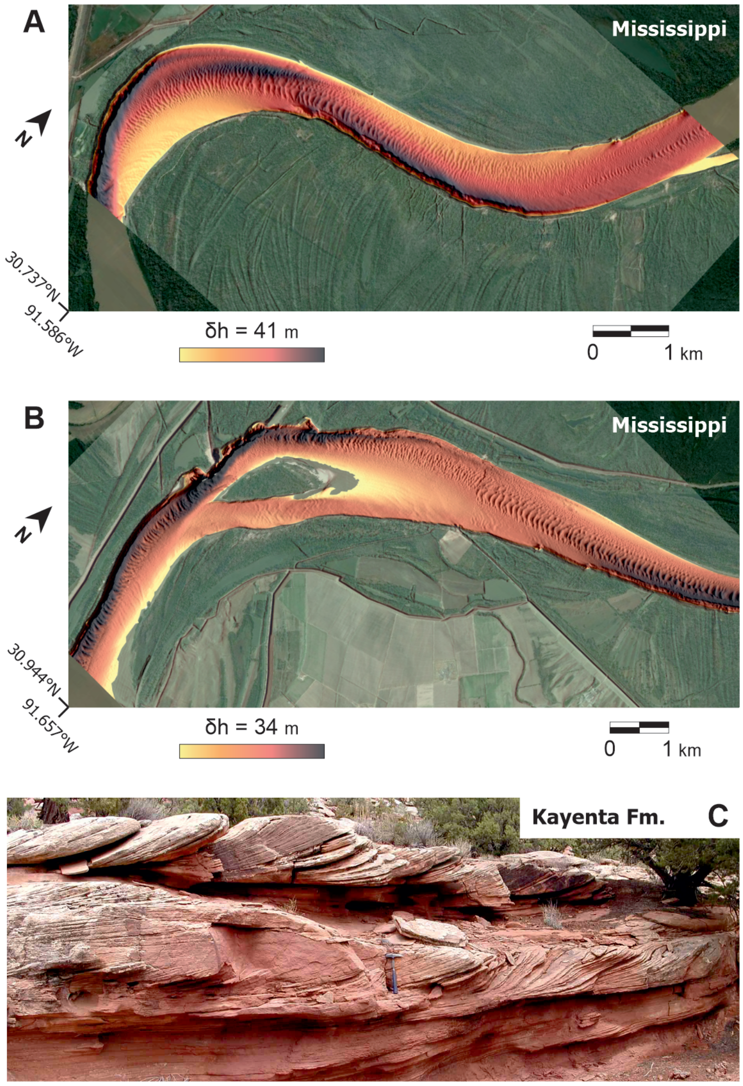

A
Mississippi
N
30.737°N
91.586°W
δh = 41 m
0
1 km
B
Mississippi
N
30.944°N
91.657°W
δh = 34 m
0
1 km
Kayenta Fm.
C

fig 1.tif

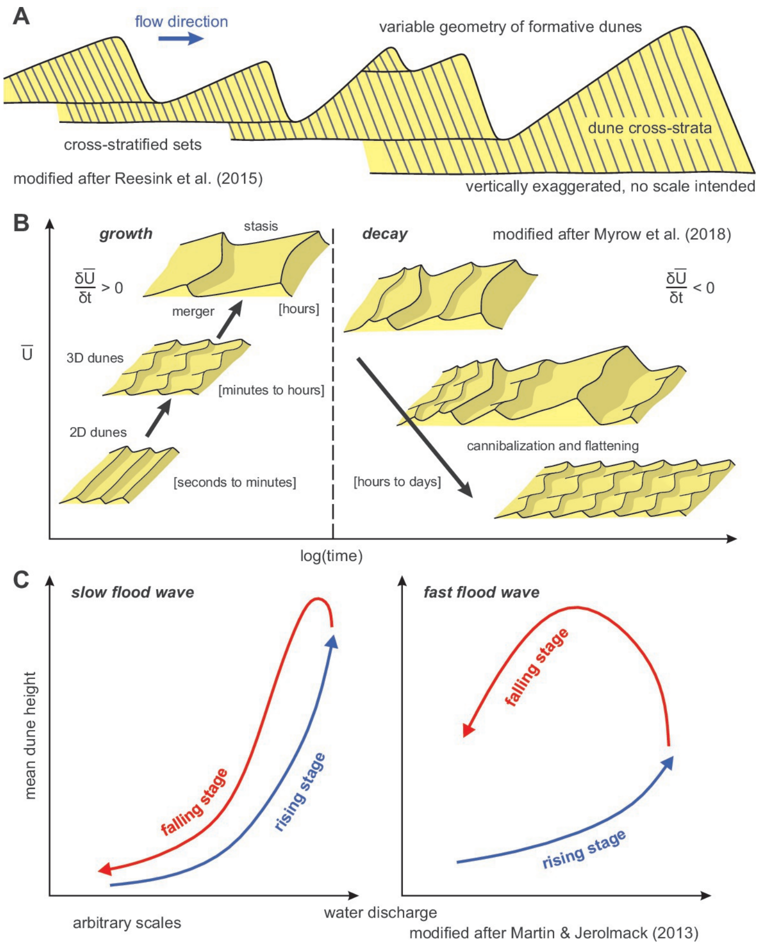
A
flow direction
variable geometry of formative dunes
cross-stratified sets
dune cross-strata
modified after Reesink et al. (2015)
vertically exaggerated, no scale intended
B
growth
stasis
decay
modified after Myrow et al. (2018)
δŪ/δt > 0
δŪ/δt < 0
merger
[hours]
3D dunes
[minutes to hours]
2D dunes
[seconds to minutes]
cannibalization and flattening
[hours to days]
Ū
log(time)
C
slow flood wave
fast flood wave
mean dune height
falling stage
rising stage
arbitrary scales
water discharge
modified after Martin & Jerolmack (2013)

fig 2.eps

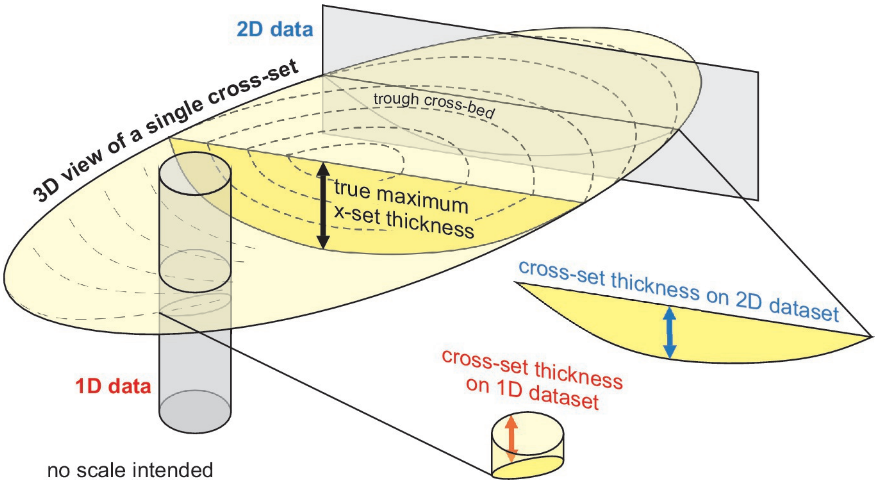
2D data
3D view of a single cross-set
trough cross-bed
true maximum
x-set thickness
cross-set thickness on 2D dataset
cross-set thickness
on 1D dataset
1D data
no scale intended

fig 3.eps

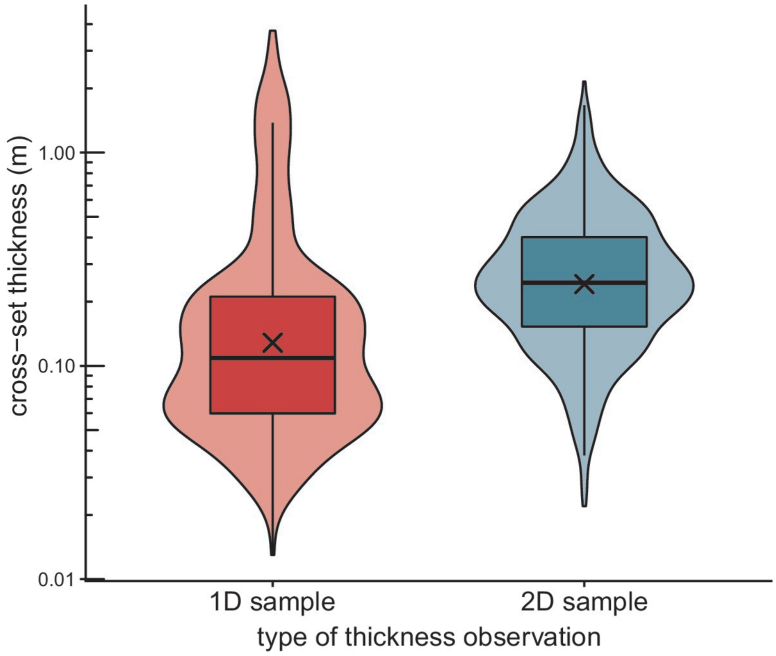
cross−set thickness (m)
1.00
0.10
0.01
1D sample
2D sample
type of thickness observation

fig 4.eps

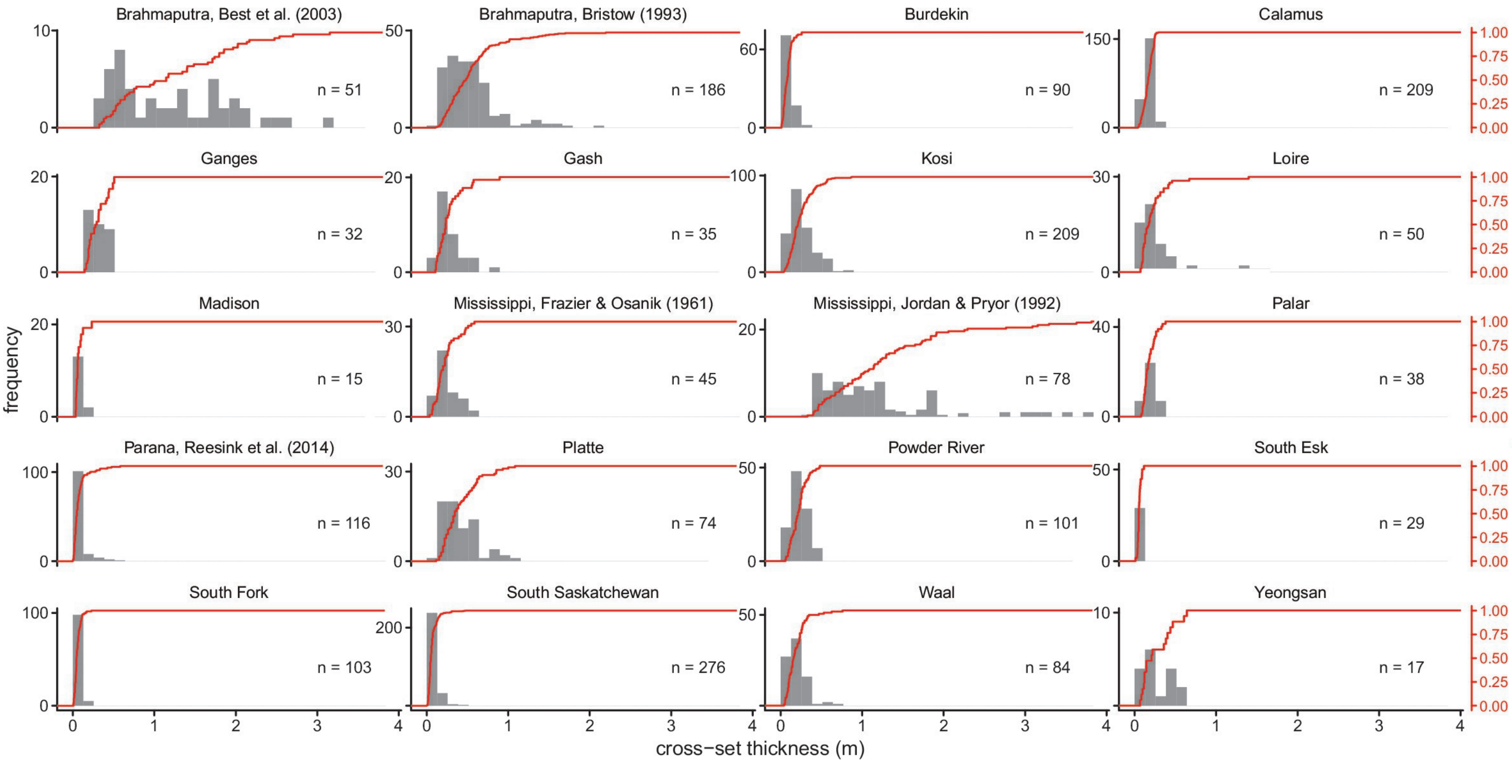
Brahmaputra, Best et al. (2003)
Brahmaputra, Bristow (1993)
Burdekin
Calamus
Ganges
Gash
Kosi
Loire
Madison
Mississippi, Frazier & Osanik (1961)
Mississippi, Jordan & Pryor (1992)
Palar
Parana, Reesink et al. (2014)
Platte
Powder River
South Esk
South Fork
South Saskatchewan
Waal
Yeongsan
n = 51
n = 186
n = 90
n = 209
n = 32
n = 35
n = 209
n = 50
n = 15
n = 45
n = 78
n = 38
n = 116
n = 74
n = 101
n = 29
n = 103
n = 276
n = 84
n = 17
frequency
cumulative density
cross−set thickness (m)

fig 5.eps

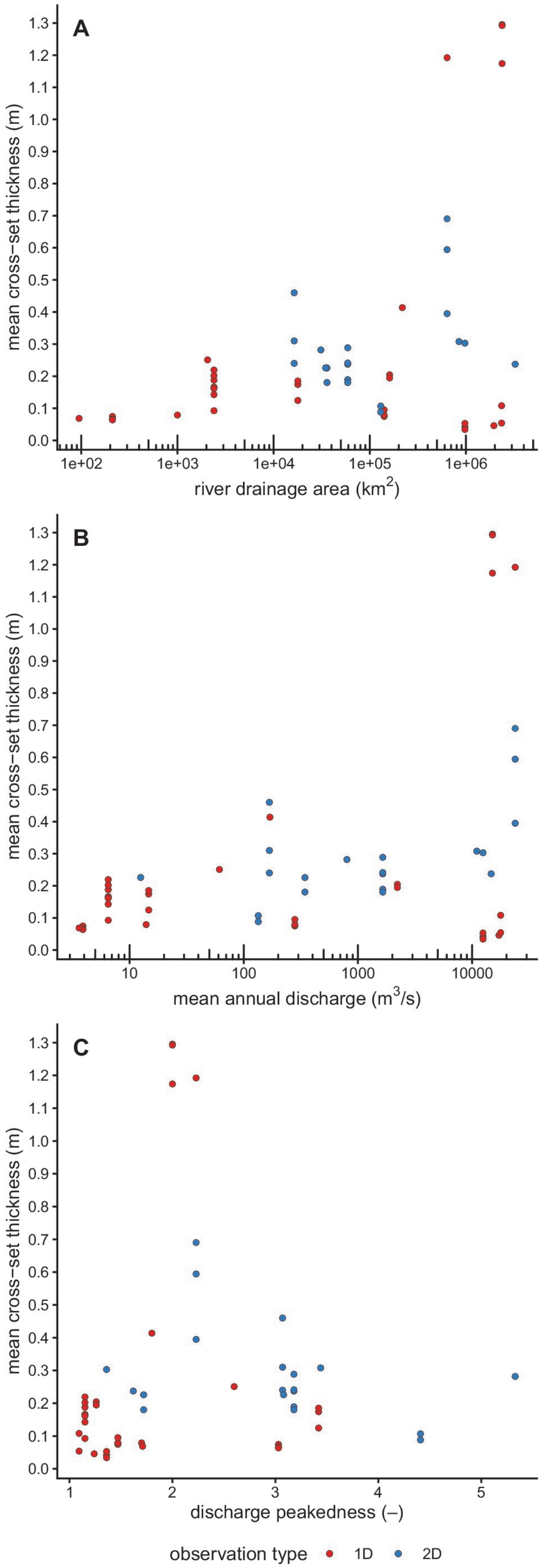
A
mean cross−set thickness (m)
river drainage area (km^2)
1e+02
1e+03
1e+04
1e+05
1e+06
B
mean annual discharge (m^3/s)
10
100
1000
10000
C
discharge peakedness (–)
observation type
1D
2D

fig 6.eps

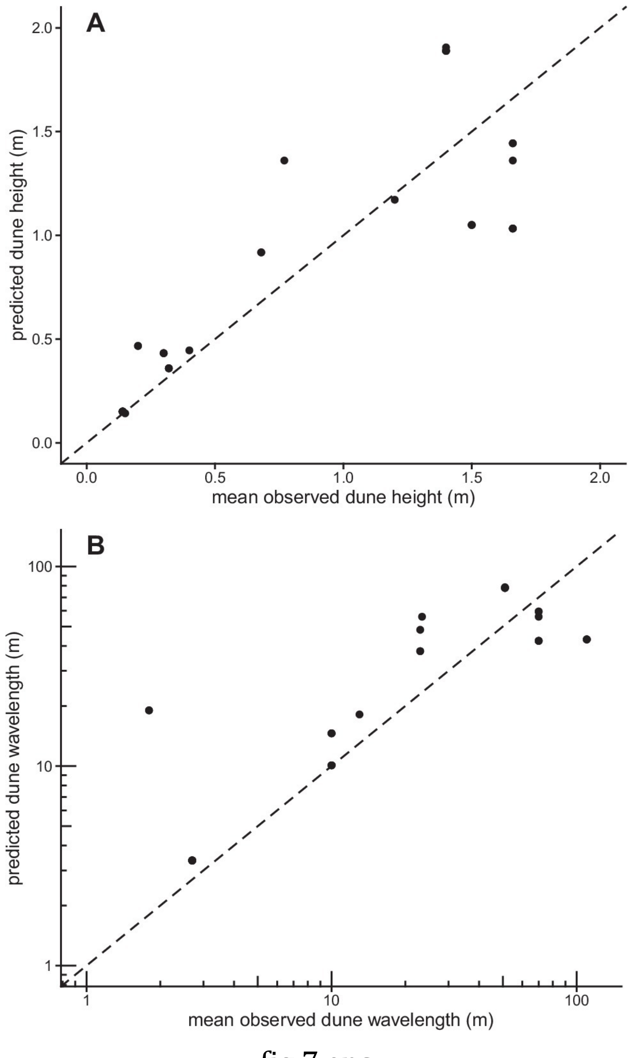
A
predicted dune height (m)
mean observed dune height (m)
0.0
0.5
1.0
1.5
2.0
B
predicted dune wavelength (m)
mean observed dune wavelength (m)
1
10
100

fig 7.eps

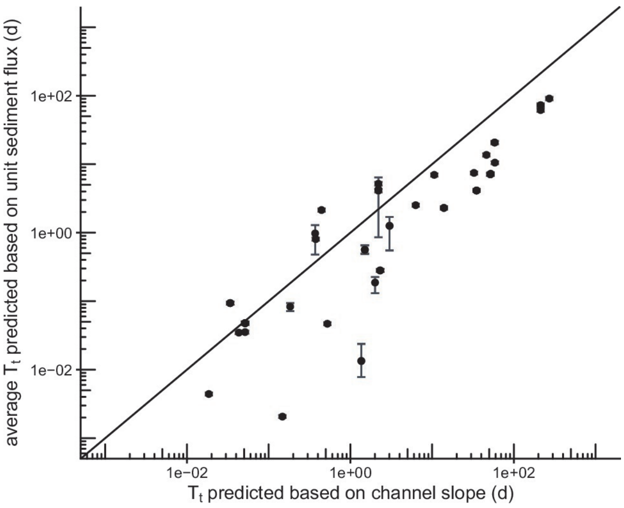

average T_t predicted based on unit sediment flux (d)
1e+02
1e+00
1e-02
1e-02
1e+00
1e+02
T_t predicted based on channel slope (d)

fig 8.eps

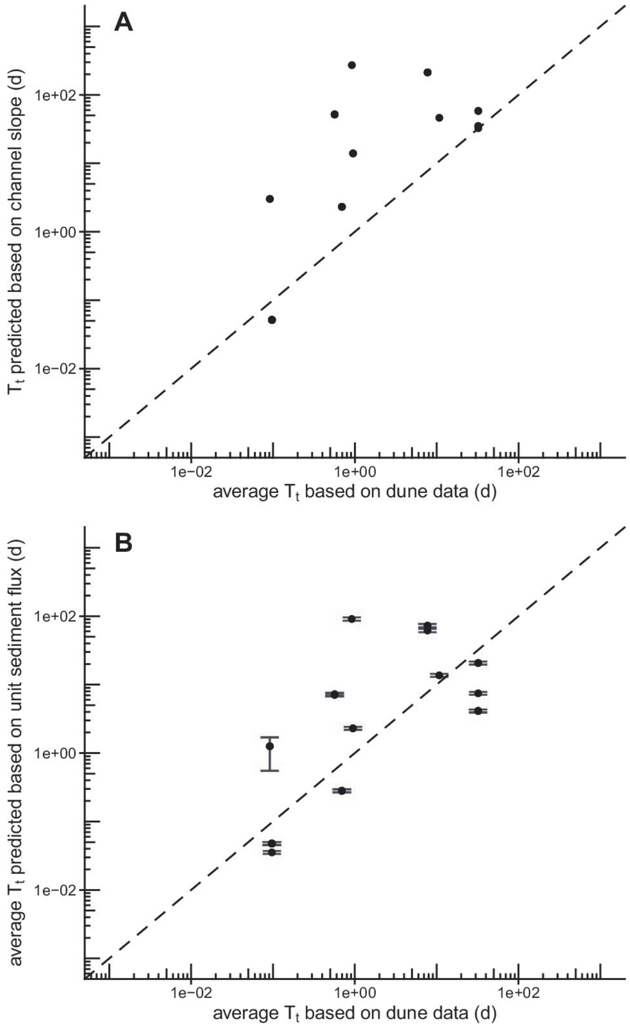
A
T t predicted based on channel slope (d)
1e+02
1e+00
1e-02
average T t based on dune data (d)
B
average T t predicted based on unit sediment flux (d)
1e+02
1e+00
1e-02
average T t based on dune data (d)

fig 9.eps

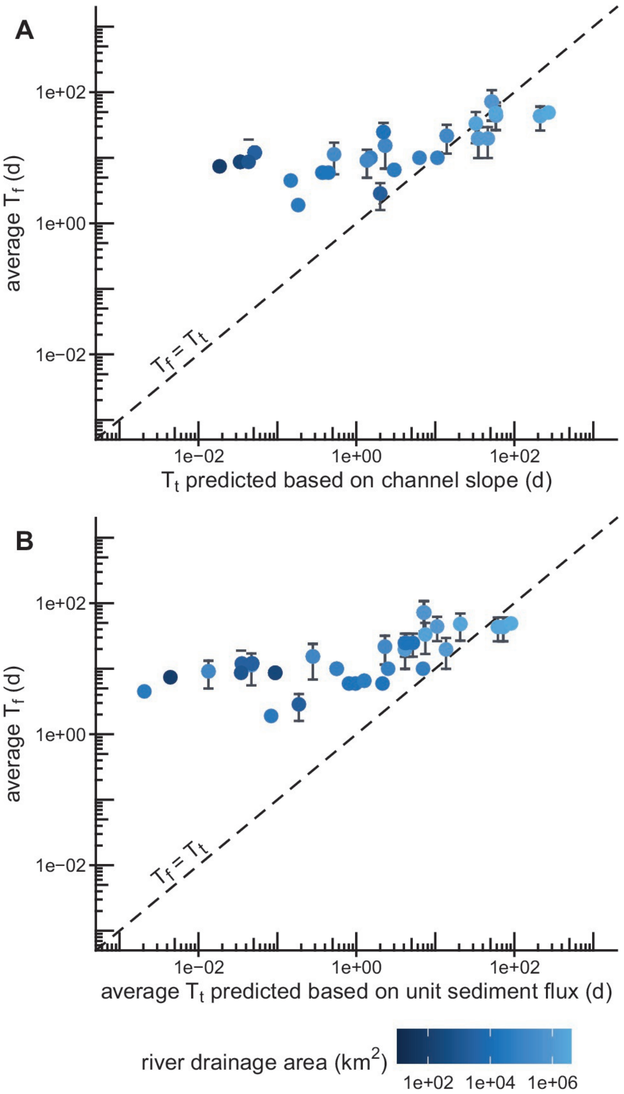
A
average T_f (d)
1e+02
1e+00
1e−02
$T_f = T_t$
1e−02
1e+00
1e+02
T_t predicted based on channel slope (d)
B
average T_f (d)
1e+02
1e+00
1e−02
$T_f = T_t$
1e−02
1e+00
1e+02
average T_t predicted based on unit sediment flux (d)
river drainage area (km^2)
1e+02
1e+04
1e+06

fig 10.eps

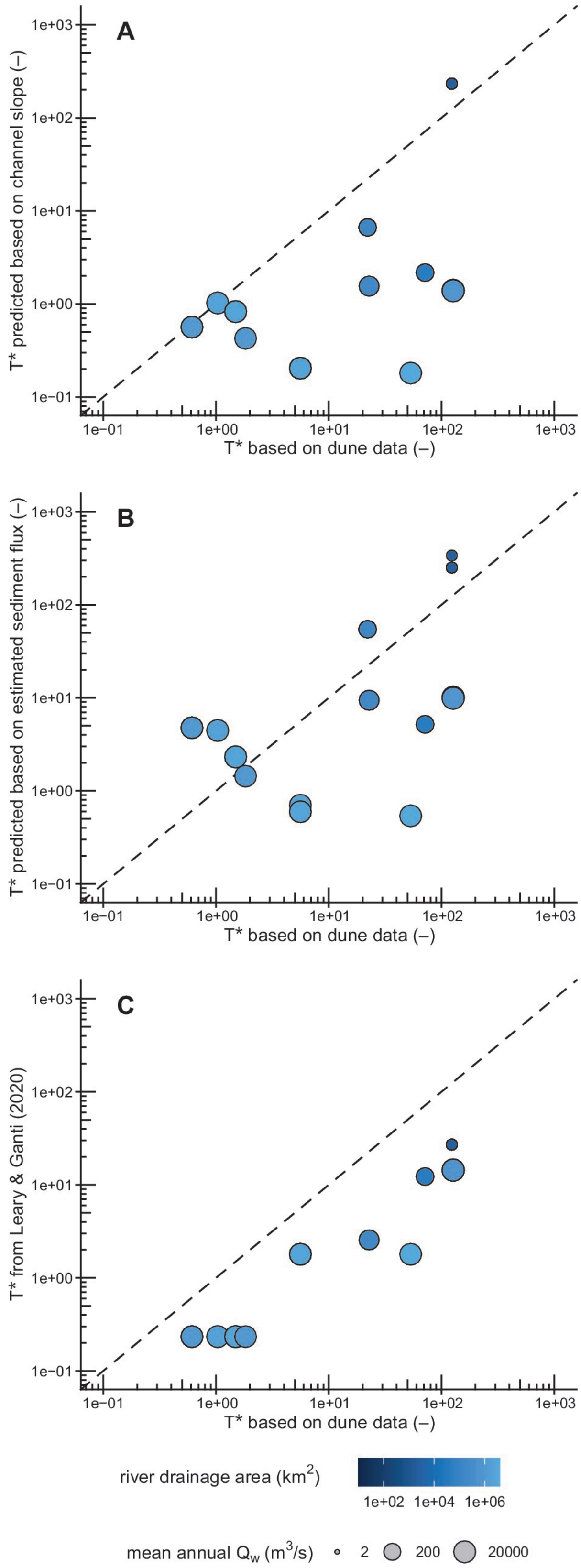
A
B
C
1e+03
1e+02
1e+01
1e+00
1e−01
1e−01
1e+00
1e+01
1e+02
1e+03
T* predicted based on channel slope (–)
T* predicted based on estimated sediment flux (–)
T* from Leary & Ganti (2020)
T* based on dune data (–)
river drainage area (km2)
1e+02 1e+04 1e+06
mean annual Qw (m3/s)
2
200
20000

fig 11.eps

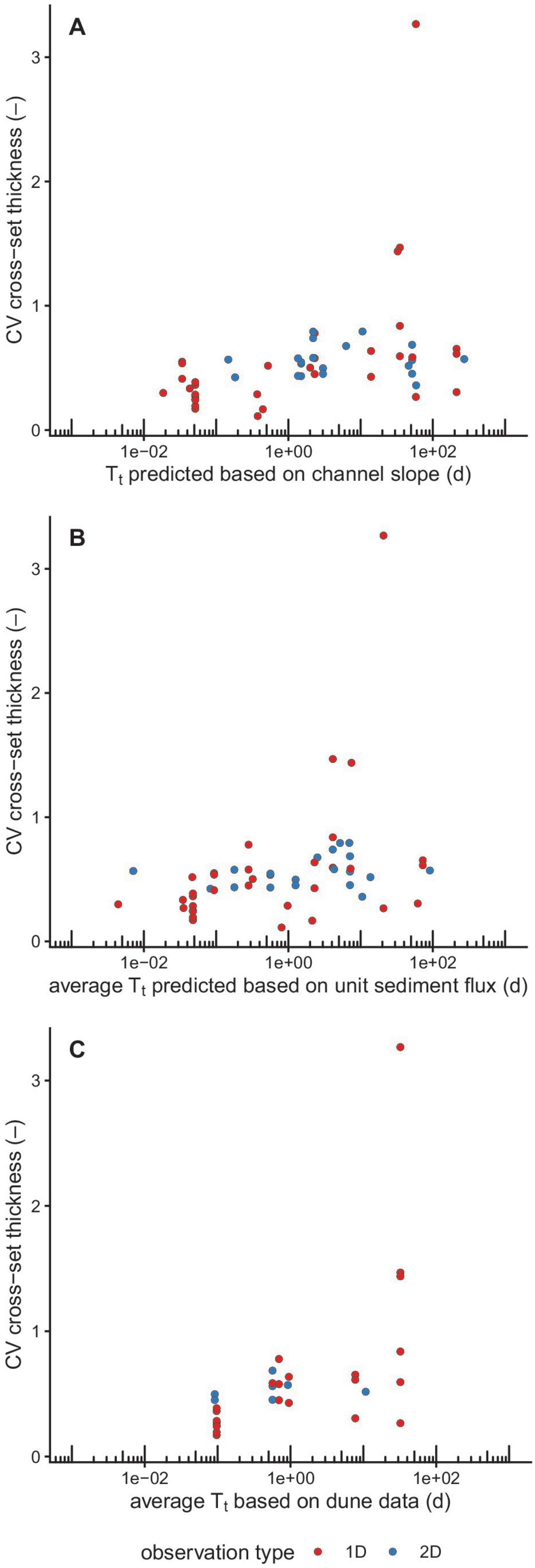
A
CV cross−set thickness (−)
Tt predicted based on channel slope (d)
B
CV cross−set thickness (−)
average Tt predicted based on unit sediment flux (d)
C
CV cross−set thickness (−)
average Tt based on dune data (d)
0
1
2
3
1e−02
1e+00
1e+02
observation type
1D
2D

fig 12.eps

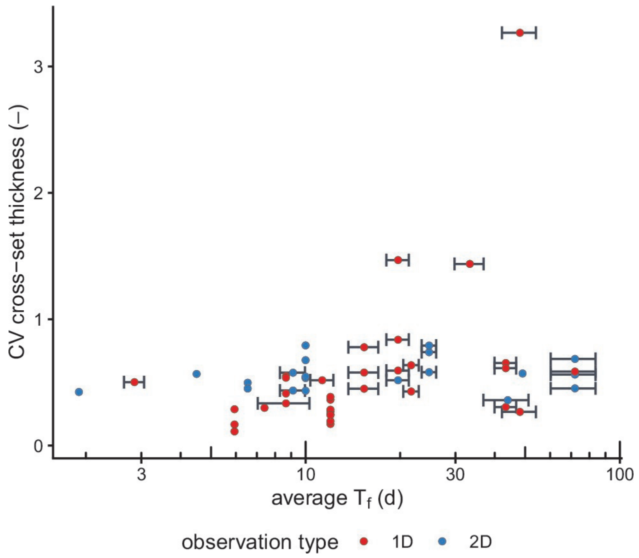

CV cross−set thickness (−)
3
2
1
0
3
10
30
100
average T_f (d)
observation type
1D
2D

fig 13.eps

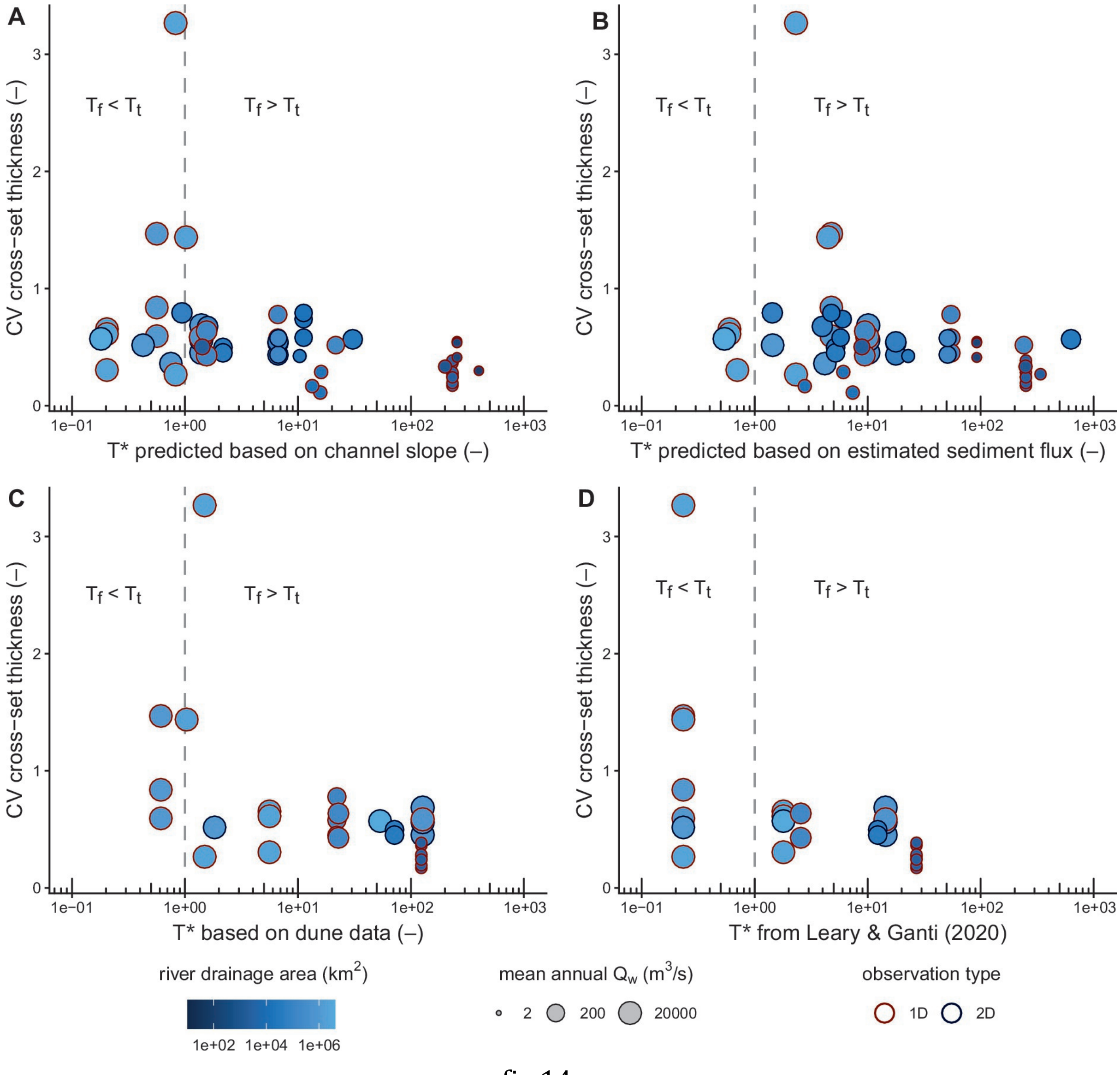
A
B
C
D
$T_f < T_t$
$T_f > T_t$
CV cross−set thickness (−)
T* predicted based on channel slope (–)
T* predicted based on estimated sediment flux (–)
T* based on dune data (–)
T* from Leary & Ganti (2020)
1e−01
1e+00
1e+01
1e+02
1e+03
river drainage area (km^2)
1e+02 1e+04 1e+06
mean annual Q_w (m^3/s)
2 200 20000
observation type
1D 2D

fig 14.eps

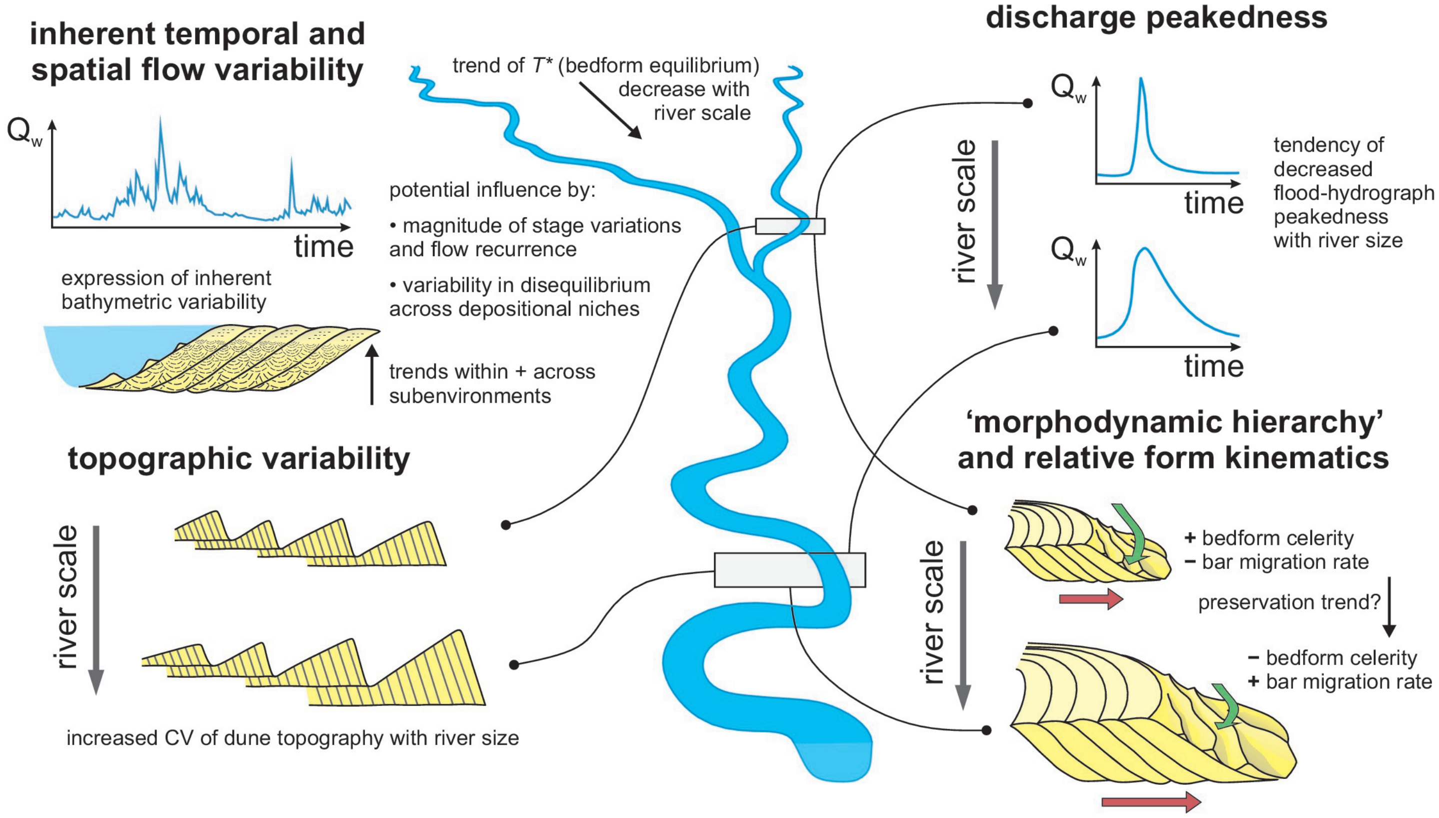
inherent temporal and spatial flow variability
Q_w
time
expression of inherent bathymetric variability
trend of T^* (bedform equilibrium) decrease with river scale
potential influence by:
• magnitude of stage variations and flow recurrence
• variability in disequilibrium across depositional niches
trends within + across subenvironments
topographic variability
river scale
increased CV of dune topography with river size
discharge peakedness
Q_w
time
river scale
tendency of decreased flood-hydrograph peakedness with river size
Q_w
time
'morphodynamic hierarchy' and relative form kinematics
river scale
+ bedform celerity
− bar migration rate
preservation trend?
− bedform celerity
+ bar migration rate

fig 15.eps